



1 **Globally significant yields of dissolved organic carbon from small watersheds of the Pacific**
2 **coastal temperate rainforest.**

3

4 Allison A. Oliver^{1,2}, Suzanne E. Tank^{1,2}, Ian Giesbrecht², Maartje C. Korver², William C.
5 Floyd^{3,4,2}, Paul Sanborn^{5,2}, Chuck Bulmer⁶, Ken P. Lertzman^{7,2}

6

7 ¹University of Alberta, Department of Biological Sciences, CW 405, Biological Sciences Bldg.,
8 University of Alberta, Edmonton, Alberta, T6G 2E9, Canada

9 ²Hakai Institute, Tula Foundation, Box 309, Heriot Bay, British Columbia, V0P 1H0, Canada

10 ³Ministry of Forests, Lands and Natural Resource Operations, 2100 Labieux Rd, Nanaimo, BC,
11 V9T 6E9, Canada

12 ⁴Vancouver Island University, 900 Fifth Street, Nanaimo, BC, V9R 5S5, Canada

13 ⁵Ecosystem Science and Management Program, University of Northern British Columbia, 3333
14 University Way, Prince George, BC, V2N 4Z9, Canada

15 ⁶BC Ministry of Forests Lands and Natural Resource Operations, 3401 Reservoir Rd, Vernon,
16 BC, V1B 2C7, Canada

17 ⁷School of Resource and Environmental Management, Simon Fraser University, TASC 1- Room
18 8405, 8888 University Drive, Burnaby, BC, V5A 1S6, Canada

19

20

21 Corresponding author: aaoliver@ualberta.ca

22

23

24

25

26

27

28

29

30

31

32

33



34 **Abstract**

35 The perhumid region of the Pacific coastal temperate rainforest of North America
36 (PCTR) is one of the wettest places on Earth and contains numerous small catchments that
37 discharge freshwater and high concentrations of dissolved organic carbon (DOC) directly to the
38 coastal ocean. However, empirical data on the flux and composition of DOC exported from these
39 watersheds is scarce. We established monitoring stations at the outlets of seven catchments on
40 Calvert and Hecate Islands, British Columbia, which represent the rain dominated outer-coast
41 region of the PCTR. Over several years, we measured stream discharge, stream water DOC
42 concentration, and stream water dissolved organic matter (DOM) composition. Discharge and
43 DOC concentrations were used to calculate DOC fluxes and yields, and DOM composition was
44 examined using absorbance and fluorescence spectroscopy, including parallel factor analysis
45 (PARAFAC). The areal estimate of annual DOC yield in water year 2015 was $33.3 \text{ Mg C km}^{-2}$
46 yr^{-1} , with individual watersheds ranging from an average of $24.1\text{-}37.7 \text{ Mg C km}^{-2} \text{ yr}^{-1}$. This
47 represents some of the highest DOC yields in the world exported to the ocean. We observed
48 strong seasonality in the quantity and composition of exports, with the majority of DOC export
49 occurring during the extended wet period of the year (September-April). Stream flow from
50 catchments reacted quickly to rain inputs, resulting in rapid flushing of relatively fresh, highly
51 terrestrial-like DOM. DOC concentration and measures of DOM composition were correlated
52 with watershed attributes, including the extent of lakes and wetlands, and thickness of organic
53 and mineral soils. Our discovery of high DOC yields from these small catchments on the outer-
54 coast of the temperate rainforest is especially compelling as they represent the delivery of
55 relatively fresh, highly terrestrial organic matter directly to the coastal ocean. This suggests that



56 this coastal margin may play an important role in the global processing of carbon and in linking
57 terrestrial carbon to marine ecosystems.

58 **1. Introduction**

59 Freshwater aquatic ecosystems process and transport a significant amount of carbon
60 (Cole et al., 2007; Aufdenkampe et al., 2011; Raymond et al., 2013). Export via running waters
61 is an important mechanism in the removal of carbon from watersheds. Globally, riverine export
62 is estimated to deliver around 0.9 Pg C yr^{-1} from land to the coastal ocean (Cole et al., 2007),
63 with typically $>50\%$ quantified as dissolved organic carbon (DOC)(Meybeck, 1982; Ludwig et
64 al., 1996; Alvarez-Cobelas et al., 2010; Mayorga et al., 2010). Rivers draining coastal watersheds
65 serve as conduits of DOC from terrestrial and freshwater sources to marine environments
66 (Mulholland and Watts, 1982; Kling et al., 2000; McClelland et al., 2014) and can have
67 important implications for coastal carbon cycling, biogeochemical interactions, ecosystem
68 productivity, and food webs (Hopkinson et al., 1998; Tallis, 2009; Tank et al., 2012; Regnier et
69 al., 2013). In regions where empirical data are currently scarce, quantifying land-to-ocean DOC
70 export is a clear priority for improving the accuracy of watershed and coastal carbon models. The
71 transfer of water and organic matter from watersheds to the coastal ocean may represent an
72 important pathway for carbon cycling and ecological subsidies between ecosystems. Therefore,
73 better understanding of these linkages is needed for constraining predictions of ecosystem
74 productivity and food webs in response to perturbations such as climate change.

75 While quantifying DOC flux within and across systems is required for understanding the
76 magnitude of carbon exchange, the composition of DOC (as dissolved organic matter, or DOM)
77 is also important for determining the ecological significance of carbon exported from coastal
78 watersheds. The aquatic DOM pool is a complex mixture that reflects both source material and



79 processing along the watershed terrestrial-aquatic continuum, and as a result can show
80 significant spatial and temporal variation (Hudson et al., 2007; Fellman et al., 2009a; Graeber et
81 al., 2012; Wallin et al., 2015). Both DOC concentration and DOM composition can serve as
82 indicators of watershed characteristics (Koehler et al., 2009), hydrologic flow paths (Johnson et
83 al., 2011; Helton et al., 2015), and watershed biogeochemical processes (Emili and Price, 2013).
84 DOM composition can also influence its role in downstream processing and ecological function,
85 such as susceptibility to biological (Judd et al., 2006) and physiochemical interactions
86 (Yamashita and Jaffé, 2008).

87 The Pacific coastal temperate rainforests of North America extend from the Gulf of
88 Alaska, through British Columbia, to Northern California and span a wide range of precipitation
89 and climate regimes. The wettest part of this region is described as the “perhumid” zone and is
90 characterized by annual precipitation >1400mm, largely composed of rain and transient snow
91 (Alaback, 1996)(Fig. 1). The perhumid Pacific coastal temperate rainforest (PCTR) extends
92 from southeast Alaska through the outer coast of central British Columbia and contains forests
93 and soils that have accumulated large amounts of carbon and store substantial quantities of
94 organic matter relative to most other temperate forests (Gorham et al., 2012). Due to high
95 precipitation and close proximity to the coast, this area represents a potential hotspot for the
96 transport and metabolism of carbon across the land-to-ocean continuum, and quantifying these
97 fluxes is pertinent for understanding global carbon cycling. Previous studies have shown that
98 streams in this region can contain high concentrations of DOC (Fellman et al., 2010; D’Amore et
99 al., 2015a) and high DOC yields (D’Amore et al., 2015b; D’Amore et al., 2016) but these studies
100 have largely focused on southeast Alaska and relatively little is known about carbon exports
101 from the perhumid PCTR of British Columbia, an area of approximately 97,824 km² (calculated



102 from spatial data adapted from Wolf et al., 1995). In addition, due to the logistical challenges of
103 conducting fieldwork in this remote region, previous studies have derived DOC flux from point
104 measurements of DOC concentrations and modelled river discharge (e.g., Mayorga et al., 2010;
105 Stackpoole et al., 2016). In this study, we conduct the first field-based estimates of DOC flux
106 from relatively undeveloped perhumid Pacific coastal temperature rainforest watersheds of the
107 British Columbia outer-coast. We examine temporal and spatial trends in flux, and describe
108 compositional characteristics of DOM exported from these watersheds to the coastal ocean.
109 Finally, we describe relationships between measures of DOC quantity, DOM character, and
110 watershed attributes.

111 **2. Methods**

112 **2.1 Study Sites**

113 Study sites are located on northern Calvert Island and adjacent Hecate Island on the
114 central coast of British Columbia, Canada (Lat 51.650, Long -128.035; Fig. 1). Average annual
115 precipitation and air temperature at sea level from 1981-2010 was 3356 mm yr⁻¹ and 8.4 °C
116 (average annual min= 0.9°C, average annual max= 17.9°C) (available online at
117 <http://www.climatewna.com/>; Wang et al., 2012), with precipitation dominated by rain, and
118 winter snowpack persisting only at higher elevations. Soils overlying the granodiorite bedrock
119 (Roddick, 1996) are usually < 1 m thick, and have formed in sandy colluvium and patchy
120 morainal deposits, with limited areas of coarse glacial outwash. Chemical weathering and
121 organic matter accumulation in the cool, moist climate have produced soils dominated by
122 Podzols and Follic Histosols, with Hemists up to 2 m thick in depressional sites (IUSS Working
123 Group WRB, 2015). The landscape is comprised of a mosaic of ecosystem types, including
124 exposed bedrock, extensive wetlands, bog forests and woodlands, with organic rich soils (Green,



125 2014; Thompson et al., 2016). Forest stands are generally short with open canopies reflecting the
126 lower productivity of the outer-coast forests compared to the rest of the perhumid rainforest
127 (Banner et al., 2005). Dominant trees are western red cedar, yellow cedar, shore pine and western
128 hemlock with composition varying across topographic and edaphic gradients. Widespread
129 understory plants include several bryophytes, salal, deer fern, and tufted clubbrush. Wetland
130 plants are locally abundant including diverse *Sphagnum* mosses and sedges. Although the
131 watersheds have no history of mining or industrial logging, archaeological evidence suggests that
132 humans have occupied this landscape for at least 13,000 years (McLaren et al., 2014). This
133 occupation has had a local effect on forest productivity near habituation sites (Trant et al., 2016)
134 and on fire regimes (Hoffman et al., 2016). We selected seven watersheds with streams draining
135 directly into the ocean (Fig. 1). These numbered watersheds (626, 693, 703, 708, 819 844, and
136 1015) range in size (3.2 to 12.8 km²) and topography (maximum elevation 160 m to 1012 m), are
137 variably affected by lakes (0.3 – 9.1% lake coverage), and – as is characteristic of the outer coast
138 – have a high degree of wetland coverage (24– 50%)(Table 1).

139 **2.2 Soils and watershed characteristics**

140 Watersheds and streams were delineated using a 3 m resolution digital elevation model
141 (DEM) derived from airborne laser scanning (LiDAR) (Gonzalez Arriola et al., 2015). We then
142 used GIS to summarize watershed characteristics for each watershed polygon and for all
143 watersheds combined (Table 1). Topographic measures were estimated from the DEM (Gonzalez
144 Arriola et al., 2015); lake and wetland cover from Province of British Columbia Terrestrial
145 Ecosystem Mapping (TEM) (Green, 2014); soil material thickness from unpublished digital soil
146 maps (Supplemental S1). We recorded thickness of organic soil material, thickness of mineral
147 soil material, and total soil depth to bedrock at a total of 353 field sites. In addition to field-



148 sampled sites, 40 sites with exposed bedrock (0 cm soil depth) were located using aerial
149 photography. Soil thicknesses were combined with a suite of topographic, vegetation, and
150 remote sensing (LiDAR and RapidEye satellite imagery) data for each sampling point and used
151 to train a random forest model (randomForest package in R; Liaw and Wiener, 2002) that was
152 used to predict soil depth values. Soil material thicknesses were then averaged for each
153 watershed (Table 1). For additional details on field site selection and methods used for soil
154 depth predictions, see Supplemental S1.1.

155 **2.3 Sample Collection and Analysis**

156 From May 2013 to July 2016, we collected stream water grab samples from each
157 watershed stream outlet every 2-3 weeks ($n_{\text{total}}=402$), with less frequent sampling (~monthly)
158 during winter (Fig. 1). All samples were filtered in the field (Millipore Millex-HP Hydrophilic
159 PES 0.45 μm) and kept in the dark, on ice until analysis. DOC samples were filtered into 60mL
160 amber glass bottles and preserved with 7.5M H_3PO_4 . Fe samples were filtered into 125mL
161 HDPE bottles and preserved with 8M HNO_3 . DOC and Fe samples were analyzed at the BC
162 Ministry of the Environment Technical Services Laboratory (Victoria, BC, Canada). DOC
163 concentrations were determined on a TOC analyzer (Aurora 1030; OI-Analytical) using wet
164 chemical oxidation with persulfate followed by infrared detection of CO_2 . Fe concentrations
165 were determined on a dual-view ICP-OES spectrophotometer (Prodigy; Teledyne Leeman Labs)
166 using a Seaspray pneumatic nebulizer.

167 In May 2014, we began collecting stream samples for stable isotopic composition of $\delta^{13}\text{C}$
168 in DOC ($\text{DO}\delta^{13}\text{C}$; $n=173$) and optical characterization of DOM using absorbance spectroscopy
169 ($n=259$). Beginning in January 2016, we also analyzed samples using fluorescence
170 spectroscopy (see section 2.6). Samples collected for $\text{DO}\delta^{13}\text{C}$ were filtered into 40mL EPA glass



171 vials and preserved with H_3PO_4 . $\text{DO}\delta^{13}\text{C}$ samples were analyzed at GG Hatch Stable Isotope
172 Laboratory (Ottawa, ON, Canada) using high temperature combustion (TIC-TOC Combustion
173 Analyser Model 1030; OI Analytical) coupled to a continuous flow isotope ratio mass
174 spectrometry (Finnigan Mat DeltaPlusXP; Thermo Fischer Scientific)(Lalonde et al. 2014).
175 Samples analyzed for optical characterization using absorbance and fluorescence were filtered
176 into 125mL amber HDPE bottles and analyzed at the Hakai Institute (Calvert Island, BC,
177 Canada) within 24 hours of collection.

178 **2.4 Hydrology: Precipitation and Stream Discharge**

179 We measured precipitation using a TB4-L tipping bucket rain gauge with a 0.2mm
180 resolution (Campbell Scientific Ltd.) located in watershed 708 (elevation= 16m a.s.l). The rain
181 gauge was calibrated twice per year using a Field Calibration Device, model 653 (HYQUEST
182 Solutions Ltd).

183 We determined continuous stream discharge for each watershed by developing stage
184 discharge rating curves at fixed hydrometric stations situated in close proximity to each stream
185 outlet. Sites were located above tidewater influence and were selected based on favourable
186 conditions (i.e., channel stability and stable hydraulic conditions) for the installation and
187 operation of pressure transducers to measure stream stage. From August 2014 to May 2016 (21
188 months), we measured stage every 5 minutes using an OTT PLS –L (OTT Hydromet, Colorado,
189 USA) pressure transducer (0-4m range SDI-12) connected to a CR1000 (Campbell Scientific,
190 Edmonton, Canada) data logger. Stream discharge was measured over various intervals using
191 either the velocity area method (for flows $< 0.5 \text{ m}^3\text{s}^{-1}$; ISO Standard 9196:1992, ISO Standard
192 748:2007) or salt dilution (for flows $> 0.5 \text{ m}^3\text{s}^{-1}$; Moore, 2005). Rating curves were developed
193 using the relationship between stream stage height and stream discharge (Supplemental S2).



194 **2.5 DOC flux**

195 From October 1, 2014 to April 30, 2016, we estimated DOC flux for each watershed
196 using measured DOC concentrations ($n=224$) and continuous discharge recorded at 15-minute
197 intervals. The watersheds in this region respond rapidly to rain inputs and as a result DOC
198 concentrations are highly variable. To address this variability, routine DOC concentration data
199 (as described in section 2.2) were supplemented with additional grab samples ($n=21$) collected
200 around the peak of the hydrograph during several high flow events throughout the year. We
201 performed watershed-specific estimates of DOC flux using the “rloadest” package (Lorenz et al.,
202 2015) in R (version 3.2.5, R Core Team, 2016), which replicates functions developed in the U.S.
203 Geological Survey load-estimator program, LOADEST (Runkel et al., 2004). LOADEST is a
204 multiple-regression adjusted maximum likelihood estimation model that calibrates a regression
205 between measured constituent values and stream flow across seasons and time and then fits it to
206 combinations of coefficients representing nine predetermined models of constituent flux. To
207 account for potentially small sample size, the best model was selected using the second order
208 Akaike Information Criterion (AICc). Input data were log-transformed to avoid bias and centered
209 to reduce multicollinearity. For additional details on model selection, see Supplemental Table
210 S3.1.

211 **2.6 Optical characterization of DOM**

212 Prior to May 2014, absorbance measures of water samples ($n=99$) were conducted on a
213 Varian Cary-50 (Varian, Inc.) spectrophotometer at the BC Ministry of the Environment
214 Technical Services Laboratory (Victoria, BC, Canada) and used to determine specific UV
215 absorption at 254 nm ($SUVA_{254}$). After May 2014, we determined optical characterization of
216 DOM by absorbance and fluorescence spectroscopy at the Hakai Institute field station (Calvert



217 Island, BC, Canada) using an Aqualog fluorometer (Horiba Scientific, Edison, New Jersey,
218 USA). Samples were run in 1 cm quartz cells and strongly absorbing samples were diluted prior
219 to analysis to avoid excessive inner filter effects (Lakowicz, 1999). We used absorbance scans
220 to determine $SUVA_{254}$ as well as the spectral slope ratio (S_R). $SUVA_{254}$ has been shown to
221 positively correlate with increasing molecular aromaticity associated with the fulvic acid fraction
222 of DOM (Weishaar et al., 2003), and is calculated by dividing the Decadic absorption coefficient
223 at 254 nm by DOC concentration (mg C L^{-1}). To account for potential Fe interference with
224 absorbance values, we corrected $SUVA_{254}$ values by Fe concentration according the method
225 described in Poulin et al., (2014). S_R has been shown to negatively correlate with molecular
226 weight (Helms et al., 2008), and is calculated as the ratio of the spectral slope from 275 nm to
227 295 nm ($S_{275-295}$) to the spectral slope from 350 nm to 400 nm ($S_{350-400}$).

228 We measured excitation and emission spectra (as excitation emission matrices, EEMs) on
229 samples every three weeks from January to July 2016 (n= 63) and used the Horiba Aqualog to
230 apply the appropriate instrument corrections for excitation and emission, inner filter effects, and
231 Raman signal calibration. We calculated the Fluorescence Index and Freshness Index for each
232 EEM. The Fluorescence Index is often used to indicate DOM source, where higher values are
233 more indicative of microbial-derived sources of DOM and lower values indicate more terrestrial-
234 derived sources (McKnight et al., 2001), and is calculated as the ratio of emission intensity at
235 450 nm to 500 nm, at an excitation of 370 nm. The Freshness Index is used to indicate the
236 contribution of autochthonous or recently microbial-produced DOM, with higher values
237 suggesting greater autochthony (i.e., microbial inputs), and is calculated as the ratio of emission
238 intensity at 380 nm to the maximum emission intensity between 420 nm and 435 nm, at
239 excitation 310 nm (Wilson and Xenopoulos, 2009).



240 To further characterize features of DOM composition, we performed PARAFAC analysis
241 using EEMs data within the drEEM toolbox for Matlab (Mathworks, MA, USA) (Murphy et al.,
242 2013). PARAFAC is a statistical technique used to decompose the complex mixture of the
243 fluorescing DOM pool into quantifiable, individual components (Stedmon et al., 2003). We
244 detected a total of six unique components, and validated the model using core consistency and
245 split-half analysis (Murphy et al., 2013; Stedmon and Bro, 2008). Components with similar
246 spectra from previous studies were identified using the online fluorescence repository,
247 OpenFluor (Murphy et al., 2014), and additional components with similar peaks were identified
248 through literature review. Since the actual chemical structure of fluorophores is unknown, we
249 used the concentration of each fluorophore as maximum fluorescence of excitation and emission
250 in Raman Units (F_{\max}) to derive the percent contribution of each fluorophore component to total
251 fluorescence.

252 **2.7 Data analysis and statistics**

253 We evaluated relationships between stream water DOC and watershed characteristics by
254 relating DOC concentration and measures of DOM character to catchment attributes using
255 redundancy analysis (RDA; type 2 scaling) in the package rdaTest (Legendre and Durand, 2014)
256 in R (version 3.2.2, R Core Team, 2015). To maximize the amount of information available, we
257 performed RDA analysis on samples collected from January to July 2016, and therefore included
258 all parameters of optical characterization (i.e., all PARAFAC components and spectral indices).
259 We assessed the collinearity of DOM compositional variables using a variance inflation factor
260 (VIF) criteria of > 10 , which resulted in the removal of PARAFAC components C2, C3, and C5
261 prior to RDA analysis. Catchment attributes for each watershed included average slope, percent
262 area of lakes, percent area of wetlands, average depth of mineral soil, and average depth of



263 organic soil. Relationships between variables were linear, so no transformations were necessary
264 and variables were standardized prior to analysis. To account for repeat monthly measures per
265 watershed and potential temporal correlation associated with monthly sampling, we included
266 sample month as a covariable (“partial-RDA”). To test whether the RDA axes significantly
267 explained variation in the dataset, we compared permutations of residuals using ANOVA (9,999
268 iterations; test.axes function of rdaTest).

269 3. Results

270 3.1 Hydrology

271 Annual precipitation for both water years (WY2015= 2661 mm; WY2016= 2587 mm),
272 was lower than the predicted historical mean annual precipitation estimated at the location of our
273 rain gauge (Fig. 1), which was approximately 2890 mm yr⁻¹ for the years 1981-2010 (Wang et
274 al., 2012; available at <http://www.climatewna.com/>). It is worth noting that annual precipitation
275 at our rain gauge location (elevation = 16 m) is substantially lower than the average amount
276 received at higher elevations, which for years 1981-2010 was approximately 5027 mm yr⁻¹ at an
277 elevation of 1000m within our study area. Annually, this area receives a very high amount of
278 annual rainfall relative to most regions of the world (<http://data.worldbank.org>) but also
279 experiences strong seasonal variation, with an extended wet period from fall through spring, and
280 a much shorter, typically drier period during summer. In WY2015 and WY2016, 86-88% of the
281 annual precipitation on Calvert Island occurred during the 8-months of wetter and cooler weather
282 between September and April (~75% of the year), designated the “wet period” (WY2015 wet=
283 2388 mm, average air temp= 7.97°C; WY2016 wet= 2235 mm; average air temp= 7.38°C). The
284 remaining annual precipitation occurred during the drier and warmer summer months of May –
285 August, designated the “dry period” (WY2015 dry= 314 mm, average air temp= 13.4°C;



286 WY2016 dry= 352 mm, average air temp= 13.1°C). Overall, although WY2015 was slightly
287 wetter than WY2016, the two years were comparable in relative precipitation during the wet
288 versus dry periods.

289 Stream discharge (Q) responded rapidly to rain events and, as a result, closely tracked
290 patterns in total precipitation, and exhibited clear seasonal patterns (Fig. 2). Similar to
291 precipitation data, higher Q occurred during the wet versus the dry period. Total Q for all
292 watersheds combined was 22% greater (range for individual watersheds= 4% to 27% greater in
293 WY2015 versus WY2016) for the wet period of WY2015 (total Q= $223.02 * 10^6$; range= $5.13 * 10^6 - 111.51 * 10^6$ m³) compared to the total Q for all watersheds in the wet period of WY2016 (total Q= $182.89 * 10^6$; range= $4.17 * 10^6 - 91.45 * 10^6$ m³).

296 **3.2 Temporal and spatial patterns in DOC concentration and DOC flux**

297 Stream waters were high in DOC concentration relative to the global average
298 concentrations in freshwater discharged directly to the ocean (average DOC for Calvert and
299 Hecate Islands = 10.4 mg L^{-1} , std= 3.8; average global DOC= $\sim 6 \text{ mg L}^{-1}$)(Meybeck, 1982;
300 Harrison et al., 2005) (Table 1; Fig. 3). Q-weighted average DOC concentrations were higher
301 than the average measured DOC concentrations (11.1 mg L^{-1} , Table 2), and also resulted in
302 slightly different ranking of the watersheds for highest to lowest DOC concentration. Within
303 watersheds, flow-weighted DOC concentrations ranged from a low of 8.4 mg L^{-1} (watershed
304 693) to a high of 19.3 mg L^{-1} (watershed 819). Variability tended to be higher in watersheds
305 where DOC concentration was also high (watersheds 626, 819, and 844) and lower in watersheds
306 with greater lake area (watersheds 1015 and 708)(Table 2; box plots, Figure 3). Low DOC
307 concentration and variability in DOC concentrations were also observed for watershed 703,
308 which lacks a high lake area but had the highest water yield as a result of having both the largest



309 total watershed area and the highest maximum elevation (resulting in greater precipitation
310 delivered to the catchment). On an annual basis, DOC concentrations decreased through the wet
311 period, and then increased through the dry period.

312 Annual and monthly watershed DOC yields are presented in Table 1. For the total period
313 of available Q (October 1, 2014 - April 30, 2016; 19 months), areal (all watersheds) DOC yield
314 was $52.3 \text{ Mg C km}^{-2}$ (95% CI= 45.7 to $68.2 \text{ Mg C km}^{-2}$). For the complete water year of 2015,
315 areal annual DOC yield was $33.3 \text{ Mg C km}^{-2} \text{ yr}^{-1}$ (95% CI= 28.9 to $38.1 \text{ Mg C km}^{-2} \text{ yr}^{-1}$). Total
316 monthly rainfall was strongly correlated with monthly DOC yield (Fig. 4), and average monthly
317 yield for the wet period ($3.35 \text{ Mg C km}^{-2} \text{ mo}^{-1}$; 95% CI= 2.94 to $4.40 \text{ Mg C km}^{-2} \text{ mo}^{-1}$) was much
318 greater than average monthly yield during the dry period ($0.50 \text{ Mg C km}^{-2} \text{ mo}^{-1}$; 95% CI= 0.41 to
319 $0.62 \text{ Mg C km}^{-2} \text{ mo}^{-1}$).

320 On a per-watershed basis, DOC load generally increased with total watershed area, but
321 this pattern was not maintained for DOC yield (Fig. 5). During WY2015, per-watershed yields
322 ranged from 24.1 to $43.6 \text{ Mg C km}^{-2}$ (Table 1). Overall, 94% of the export in WY2015 occurred
323 during the wet period, with a clear decrease in area-normalized export between WY2015 and
324 WY2016 (Fig. 5).

325 3.3 Temporal and spatial patterns in DOM composition

326 Iron-corrected SUVA_{254} values were relatively high compared to the range typically
327 found in surface waters (average SUVA_{254} for Calvert and Hecate Islands= $4.42 \text{ L mg}^{-1} \text{ m}^{-1}$, std=
328 0.46; range of SUVA_{254} in surface waters = 1.0 to $5.0 \text{ L mg}^{-1} \text{ m}^{-1}$)(Spencer et al., 2012)
329 suggesting DOM exported from these watersheds is comprised of highly aromatic carbon
330 compounds. Values of SUVA_{254} were relatively consistent across watersheds, however there was
331 a strong seasonal trend that countered seasonal trends in DOC concentration; SUVA_{254} values



332 generally increased over the wet period and decreased over the dry period (Fig. 3). In contrast to
333 $SUVA_{254}$, S_R showed clear variation between watersheds, indicating systematic differences in the
334 average molecular weight of the DOM pool between watersheds. Overall values of S_R were low
335 (average $S_R = 0.78$, $std = 0.04$; $range = 0.71$ to 0.89) compared to the range typically observed in
336 surface waters. This suggests that DOM was of high molecular weight, i.e., comprised of larger
337 molecules that have not been chemically or biologically degraded through processes such as
338 microbial utilization or photodegradation, and therefore are potentially more biologically
339 available (Amon and Benner, 1996). Similar to $SUVA_{254}$, S_R also appeared to fluctuate
340 seasonally, with values decreasing (increasing in molecular weight) during the wet season and
341 showing higher, more variable values during the dry season.

342 The stable isotopic composition of dissolved organic carbon ($DO\delta^{13}C$) was relatively
343 similar across watersheds (average $DO\delta^{13}C = -26.53\%$, $std = 0.36$; $range = -27.67\%$ to -24.89%)
344 and exhibited some seasonal variation; values became slightly less depleted throughout the wet
345 period relative to the dry period. Values for $DO\delta^{13}C$ suggested that terrestrial carbon sources
346 originating from C3 plants and soils were the dominant input to catchment stream water DOM
347 (Finlay and Kendall, 2007).

348 **3.4 Characterization of DOM- PARAFAC**

349 PARAFAC analysis indicated that terrestrial-derived organic carbon dominated spectral
350 signatures across watersheds and across time. Six fluorescence components were identified
351 through PARAFAC (“C1” through “C6”)(Table 2). Additional details on PARAFAC results are
352 provided in Supplemental Table S4.1, Fig. S4.2, and Fig. S4.3. Of the six components, four were
353 found to have close spectral matches in the OpenFluor database (C1, C3, C5, C6; minimum
354 similarity score > 0.95), while the other two (C2 and C4) were found to have similar peaks



355 represented in the literature. The first four components (C1 through C4) are described as
356 terrestrial-derived and comprised the majority of total fluorescence across all watersheds (Fig. 6).
357 C1 was by far the most dominant component in terms of percent contribution to total
358 fluorescence, suggesting a high and consistent supply of humic-like terrestrial material that is
359 relatively fresh (less-processed). Of the terrestrial-like components, C1, C2, and C4 exhibited
360 similar patterns to each other in their contribution to total fluorescence (Fig. 6) (Supplemental
361 Fig. S4.4), whereas component C3 appeared inversely related to the other terrestrial-like
362 components and exhibited the lowest spatial variability in percent contribution to total
363 fluorescence. Components C5 and C6 had spectral patterns indicative of autochthonous or
364 microbial-like origins, with C6 being the only component representing a distinct protein or
365 tryptophan-like contribution. Concentrations of C5 and C6 were correlated to one another (F_{\max}
366 C5 vs. F_{\max} C6, $r^2=0.22$, $p < 0.001$), but neither appeared to covary with terrestrial components.
367 Relative to other components, C5 and C6 demonstrated the greatest variation between
368 watersheds (Supplemental Fig. S4.4). In general, the rank order of the components' percent
369 contribution to total fluorescence and variability between watersheds was maintained over time,
370 although on average percent composition of C2 and C4 was higher, and C3 was lower for
371 watersheds 819 and 844 relative to the other watersheds (Supplemental Fig. S4.4). The relative
372 importance of various components appeared consistent across the wet and dry periods, although
373 slightly more variation was observed during the dry period.

374 **3.5 Relationships between watershed characteristics and DOC exports**

375 Results of the partial-RDA (type 2 scaling) were significant in explaining variability in
376 DOM concentration and composition (semi-partial $R^2=0.33$, $F=7.90$, $p < 0.0001$) (Fig. 7). Axes 1
377 through 3 were statistically significant at $p < 0.001$, and the relative contribution of each axis to



378 the total explained variance was 47%, 30%, and 22%, respectively. Additional details on the
379 RDA test are provided in Supplemental Figs. S5.1-S5.2 and Tables S5.3 – S5.5. Axis 1 described
380 a gradient of watershed inundation from lakes versus wetlands, with lake area and mean mineral
381 soil material thickness showing a strong positive contribution, and wetlands showing a strong
382 negative contribution to this axis. The Freshness Index, Fluorescence Index, S_R and fluorescence
383 component C6 were all positively correlated with this axis, while component C4 showed a clear
384 negative correlation. Axis 2 described a subtler gradient of soil composition from greater mean
385 organic soil material thickness to greater mean mineral soil material thickness. DOC
386 concentration, $DO\delta^{13}C$, SUVA, and fluorescence component C1 all showed a strong, positive
387 correlation with Axis 2. Axis 3 described a gradient of watershed steepness, from lower gradient
388 slopes with more wetland area and thicker organic soil material to steeper slopes with less
389 developed organic horizons. Average slope contributed negatively to Axis 3 (see Supplemental
390 Table S5.5), followed by positive contributions from both percent wetland area and thickness of
391 organic soil material. $DO\delta^{13}C$ showed the most positive correlation with Axis 3, whereas
392 fluorescence components C1 and C4 showed the most negative.

393 **4. Discussion**

394 **4.1 DOC flux: High DOC yields from small catchments to the coastal ocean**

395 Freshwater DOC yields from Calvert and Hecate Island watersheds are some of the
396 highest recorded globally, and in the upper range for this region when compared to previous
397 regional predictions from global models (Mayorga et al., 2010) and DOC exports quantified for
398 southeastern Alaska (D'Amore et al., 2015a; D'Amore et al., 2016; Stackpoole et al., 2016). On
399 a global scale, DOC yields from Calvert and Hecate Island watersheds were higher than
400 estimates from many tropical rivers including the Congo River (Spencer et al., 2016),



401 Amazonian blackwater rivers (Moreira-Turcq et al., 2003; Waterloo et al., 2006) and southeast
402 Asian rivers draining virgin tropical peatlands (Baum et al., 2007), even though these types of
403 tropical rivers are often regarded as having disproportionately high carbon export compared to
404 temperate and Arctic rivers (Aitkenhead and McDowell, 2000; Borges et al., 2015).

405 While comparable DOC yields have been estimated from other high-latitude catchments
406 that receive high amounts of precipitation and contain organic soils (e.g. Naiman, 1982; Ågren et
407 al., 2007), these are typically small catchments containing low (first or second) order headwater
408 streams draining to higher order stream reaches. While headwater streams have been shown to
409 export up to 90% of the total annual carbon in stream flow (Leach et al., 2016), DOC exported
410 from headwaters and low order streams may potentially undergo significant processing before
411 reaching the ocean. In that regard, our discovery of high DOC yields from Calvert and Hecate
412 Island watersheds is especially compelling because these catchments drain directly to the ocean,
413 therefore providing a large and concentrated supply of relatively fresh terrestrial DOC directly to
414 a low DOC marine environment. Over much of the complex, incised outer coast of the perhumid
415 Pacific coastal temperate rainforest, small, rainfall-dominated catchments are the most direct
416 source of freshwater runoff to the coastal ocean (Eaton and Moore, 2010; Hill et al., 2015;
417 Royer, 1982). Our findings suggest that the small catchment of this region enable geographically
418 distributed inputs of high DOC flux directly to the coastal ocean, and that this region could
419 represent a significant biogeochemical hotspot for coastal carbon cycling.

420 Flashy stream hydrographs indicate that hydrologic residence times for Calvert and
421 Hecate Island watersheds are typically short, presumably as a result of small catchment size, high
422 drainage density, and relatively shallow soils with high hydraulic conductivity (Gibson et al.,



423 2000; Fitzgerald et al., 2003). Precipitation is a well-established driver of stream DOC export
424 (Alvarez-Cobelas et al., 2012) particularly in systems containing organic soils and wetlands
425 (Olefeldt et al., 2013; Wallin et al., 2015; Leach et al., 2016). In general, frequent high
426 precipitation events and short residence times are expected to result in pulsed exports of stream
427 DOC that is rapidly shunted downstream, thus reducing time for in-stream processing (Raymond
428 et al., 2016). Rapid runoff is presumably accompanied by rapid increases in water tables and
429 lateral movement of water through shallow soil layers rich in organic matter (Fellman et al.,
430 2009; D'Amore et al., 2015b) We observed distinct seasonality of DOC delivery to the coastal
431 ocean, which may be important for determining downstream effects on ecological processes.

432 **4.2. DOM character: Sources, variability, and implications for coastal marine foodwebs**

433 On Calvert and Hecate Islands, short catchment residence times reduce opportunities for
434 in-stream production and processing, and, in conjunction with water flowing through abundant
435 sources of DOM from organic-rich soils, wetlands, and forests, result in high quantities of
436 terrestrial DOM export from watersheds to the ocean. This is consistent with findings from
437 previous studies on DOM exports from streams draining small headwater catchments
438 (Yamashita et al., 2011), and undisturbed catchments comprised of mixed forest and wetlands
439 (e.g. Wickland et al., 2007; Fellman et al., 2009a; Spencer et al., 2010). Seasonal variability in
440 DOM composition may be attributed to differences in DOM source due to seasonal changes in
441 biological activity or as a result of shifting flow paths that affect hydrologic interactions with
442 different DOM source materials (Fellman et al., 2009b). Rising water tables can establish strong
443 hydraulic gradients that initiate and sustain prolonged increases in metrics like SUVA₂₅₄, until
444 the progressive drawdown of upland water tables constrain flow paths (Lambert et al., 2013).
445 For example, during the wet and cooler period DOM increased in aromaticity and molecular



446 weight, indicating an increase in contributions of more plant and soil-derived material as
447 saturated conditions promote the mobilization of a wide range of DOM source materials
448 (McKnight et al., 2001; Kalbitz et al., 2002). However, this trend was reversed during the dry
449 and warmer period, suggesting a shift in the source of DOM and/or increased contributions from
450 microbial products and plant exudates, and perhaps deeper flow paths that contribute to mineral
451 binding and export of older, more processed terrestrial material (McKnight et al., 2001; van Hees
452 et al., 2005). Similarly, proportions of fluorescence components were more consistent across
453 watersheds during the wet period compared to the dry period, further suggesting that water table
454 draw down and unsaturated soils lead to more diverse flow paths and interaction with different
455 sources of DOM. The interaction of sources and flow paths during wet versus dry periods may
456 have important consequences for the downstream fate of this material.

457 Biological utilization of DOM is influenced by its composition (e.g. Judd et al., 2006;
458 Fasching et al., 2014), therefore differences in the nature of DOM exports will likely alter the
459 downstream fate and ecological role of freshwater-exported DOM. The majority of the
460 fluorescent DOM pool was comprised of C1, which is described as humic-like, less-processed
461 terrestrial soil and plant material (see Table 2), and thus may represent a relatively fresh,
462 seasonally-consistent contribution of terrestrial material from streams to the coastal ecosystem.
463 This may have ecological significance as a potential subsidy for downstream microbial
464 production. In lakes, for example, pulsed contributions of less-processed humic material
465 exported from rivers have been shown to stimulate bacterial production (Bergström and Jansson,
466 2000). In comparison to the more humic fractions, the tryptophan-like component, C6, represents
467 a portion of the DOM pool comprised of a higher proportion of proteins that are preferred and
468 readily utilized by microbial communities (Stedmon and Markager, 2005). Although C6



469 represents a minor, more variable proportion of total fluorescence in comparison to the more
470 humic compounds such as C1, even a small proteinaceous fraction of the overall DOM pool can
471 play a major role in overall bioavailability and bacterial utilization of DOM (Berggren et al.,
472 2010; Guillaumette and Giorgio, 2011). While previous studies have suggested that bacteria
473 prefer autochthonous carbon sources, they also readily utilize allochthonous terrestrial DOC
474 subsidies (Bergström and Jansson, 2000; Kritzberg et al., 2004; McCallister and Giorgio, 2008),
475 enabling humic and fulvic material to potentially fuel a low but continuous level of bacterial
476 productivity after more labile sources have been consumed (Guillaumette and Giorgio, 2011).
477 Given that the small watersheds of this region export very high amounts of terrestrial DOC, there
478 is clear potential for this stream-exported DOM to provide pulsed contributions of terrestrial
479 subsidies to coastal foodwebs.

480 **4.3 Relationships between watershed attributes and exported DOM**

481 While previous studies have implicated wetlands as a major driver of DOM composition,
482 the analysis of relationships between Calvert and Hecate Island landscape attributes and variation
483 in DOM character suggests that controls on DOM composition are more nuanced than being
484 driven solely by the influence of wetlands. Ågren et al. (2008) found that when wetland area
485 comprised >10% of total catchment area, wetland DOM was the most significant driver of
486 stream DOM composition during periods of high hydrologic connectivity. Wetlands comprise an
487 average of 37% of the total area of the watersheds used in this study, so, based on Agren et al.
488 (2008) they should be a primary driver of DOC concentration and DOM composition. In our
489 study, although we observed characteristics of DOM commonly found in wetland exports,
490 wetlands do not appear to be the single leading driver of variability. Other factors, such as the
491 depth of organic and mineral soil materials, alternative DOC-source pools, and watershed



492 residence time appear to be important drivers of DOC concentration and DOM composition. In
493 these watersheds, soils with pronounced accumulations of organic matter are not restricted to
494 wetland ecosystems. While Hemists occur in the latter, which comprise 27.8% of the watersheds,
495 Follic Histosols occur on hillslopes over an additional 25.7% of the study area (Supplemental
496 S1.2). This suggests the importance of widely distributed, alternative soil DOM source-pools,
497 such as Follic Histosols and associated Podzols with thick forest floors on hillslopes, available to
498 contribute high amounts of terrestrial carbon for export.

499 Although lakes make up a relatively small proportion of the total landscape area, their
500 influence on DOM export appears to be important. The proportion of lake area can be a good
501 predictor of organic carbon loss from a catchment since lakes often increase hydrologic
502 residence times and thus increase opportunities for biogeochemical processing (Algesten et al.,
503 2004; Tranvik et al., 2009). In our study, watersheds with a larger percentage of lake area
504 exhibited lower DOC yields, and lake area was correlated with parameters that represent greater
505 autochthonous DOM production or microbial processing such as higher Freshness Index, S_R ,
506 Fluorescence Index, and higher proportions of component C6. In contrast, watersheds with a
507 high percentage of wetlands contributed a different composition of DOM than watersheds with a
508 high percentage of lakes, therefore the proportion of different landscape types, such as wetlands
509 or lakes, appears to be an important factor influencing aspects of DOM export. In addition,
510 watersheds with the slowest response to rain events had lakes close to their catchment outlet
511 (e.g., watershed 1015, data not shown) that appear to dampen the response to rain events and
512 increased residence time low in the watershed. Therefore, the relative location of wetlands and
513 lakes within the catchment and their proximity to the watershed outlet also likely plays an
514 important role in the overall composition of DOM exports.



515 Soil composition also plays a role in the quantity and character of DOM exported from
516 Calvert and Hecate Island watersheds. Organic and mineral soil materials provide different
517 environments for the production, retention, and degradation of DOM. It is generally known that
518 where peat has accumulated enough to form organic soils (Hemists), DOM is the most mobile
519 fraction of organic matter and accumulates under conditions of soil saturation and limited
520 drainage, resulting in the enrichment of poorly biodegradable, more stable humic acids
521 (Stevenson, 1994; Marschner and Kalbitz, 2003). However, on hillslopes where Follic Histosols
522 have formed under more freely drained conditions, high rates of respiration in organic soils can
523 result in further enrichment of aromatic and more complex molecules, and this material may be
524 rapidly mobilized and exported to streams (Glatzel et al., 2003). Preferential retention of certain
525 DOM fractions by sorption to mineral horizons can increase stability of the DOM pool by
526 reducing biodegradation, and is postulated as the main process by which DOM is retained in
527 forest soils (Kalbitz et al., 2005; Kaiser et al., 1997). In our study, the presence of thicker organic
528 soil material was positively correlated to higher DOC concentrations, as well as higher
529 proportions of C1, representing less processed, humic-like compounds. Steeper slopes were also
530 correlated with C1 (RDA Axis 3), suggesting that steeper slopes and adequate drainage may
531 result in the rapid mobilization of this material from organic soil horizons.

532 Changing environmental conditions, such as shifting precipitation and temperature
533 regimes, may affect future DOC fluxes. Long term patterns in DOC flux have been observed in
534 many places (e.g., Worrall et al., 2004; Borke et al., 2011; Lepistö et al., 2014) and continued
535 monitoring of this system will allow us to better understand the underlying drivers of export. For
536 example, changes in soil temperature and moisture could influence the stability of the organic
537 matter pool, as processes such as organic matter production and sorption have strong



538 relationships with temperature and oxidation state. Therefore, additional research is needed to
539 assess soil properties relevant to DOM mobility (e.g., texture, sesquioxide content), landscape
540 attributes, and flow paths for predicting DOM export in this region and the consequences of
541 shifting conditions such as those associated with altered land use or climate change.

542 **5. Conclusions**

543 Previous work has demonstrated freshwater discharge is substantial along the coastal
544 margin of the Pacific temperate rainforest, and plays an important role in processes such as ocean
545 circulation (Royer, 1982; Eaton and Moore, 2010). Our finding that small catchments in this
546 region export some of the highest yields of terrestrial DOC in the world to coastal waters
547 suggests that freshwater inputs may also influence ocean biogeochemistry and food web
548 processes through terrestrial organic matter subsidies. Our findings also suggest that this region
549 may be currently underrepresented in terms of its role in global carbon cycling. Currently, there
550 is no region-wide carbon flux model for the Pacific coastal temperate rainforest or the greater
551 Gulf of Alaska, which would quantify the importance of this region within the global carbon
552 budget. Our estimates represent the hypermaritime outer-coast zone, where subdued terrain, high
553 rainfall, ocean moderated temperatures and poor bedrock have generated a distinctive ‘bog-
554 forest’ landscape mosaic within the greater temperate rainforest (Banner et al. 2005). To quantify
555 regional scale fluxes of rainforest carbon to the coastal ocean, further research will be needed to
556 estimate DOC yields across the west-to-east, and north to south, gradients of topography,
557 climate, hydrology, soils and vegetation. Further study on the controls of DOC export from these
558 watersheds, such as the role of landscape type (e.g., different wetland and forest types within the
559 ecosystem mosaic), watershed attributes (e.g., stream connectivity, slope, etc.), and detailed
560 characterization of soils, are warranted. Coupled with current studies investigating the fate of



561 terrestrial material in ocean food webs, this work will improve our understanding of coastal
562 carbon patterns, and increase capacity for predictions regarding the ecological impacts of climate
563 change.

564

565 **Author Contributions**

566 The authors declare that they have no conflict of interest.

567 A.A. Oliver prepared the manuscript with contributions from all authors, designed analysis
568 protocols, analyzed samples, performed the modeling and analysis for dissolved organic carbon
569 fluxes, parallel factor analysis of dissolved organic matter composition, and all remaining
570 statistical analyses. S.E. Tank assisted with designing the study and overseeing laboratory
571 analyses, crafting the scope of the paper, and determining the analytical approach.

572 I. Giesbrecht led the initial DOC sampling design, helped coordinate the research team, oversaw
573 routine sampling and data management, and led the watershed characterization.

574 M.C. Korver developed the rating curves, and conducted the statistical analysis of discharge
575 measurement uncertainties and rating curve uncertainties. W.C. Floyd lead the hydrology
576 component of this project, selected site locations, installed and designed the hydrometric
577 stations, and developed the rating curves and final discharge calculations. C. Bulmer and P.
578 Sanborn collected and analyzed soil field data and prepared the digital soils map of the
579 watersheds. K.P. Lertzman conceived of and co-led the overall study of which this paper is a
580 component, helped assemble and guide the team of researchers who carried out this work,
581 provided input to each stage of the study.

582

583 **Acknowledgements**



584 This work was funded by the Tula Foundation and the Hakai Institute. The authors would like to
585 thank many individuals for their support, including Skye McEwan, Bryn Fedje, Lawren McNab,
586 Nelson Roberts, Adam Turner, Emma Myers, David Norwell, and Chris Coxson for sample
587 collection and data management, Clive Dawson and North Road Analytical for sample
588 processing and data management, Keith Holmes for creating our maps, Matt Foster for database
589 development and support, Shawn Hateley for sensor network maintenance, Jason Jackson and
590 the entire staff at Hakai Energy Solutions for installing and maintaining the sensors and
591 telemetry network. Thanks to Santiago Gonzalez Arriola for generating the watershed summaries
592 and associated data products, and Ray Brunsting for overseeing the design and implementation
593 of the sensor network and the data management system at Hakai. Additional thanks to Lori
594 Johnson and Amelia Galuska for soil mapping field assistance, and Francois Guillet for
595 PARAFAC consultation. Thanks to Dave D'Amore for inspiring the Hakai project to investigate
596 aquatic fluxes at the coastal margin and for technical guidance. Lastly, thanks to Eric Peterson
597 and Christina Munck who provided significant guidance throughout the process of designing and
598 implementing this study.

599

600 **References**

601 Ågren, A., Buffam, I., Jansson, M. and Laudon, H.: Importance of seasonality and small streams
602 for the landscape regulation of dissolved organic carbon export, *J. Geophys. Res. Biogeosci.*,
603 112(G3), doi:10.1029/2006JG000381, 2007.

604

605 Ågren, A., Buffam, I., Berggren, M., Bishop, K., Jansson, M. and Laudon, H.: Dissolved organic
606 carbon characteristics in boreal streams in a forest-wetland gradient during the transition
607 between winter and summer, *J. Geophys. Res. Biogeosci.*, 113(G3), doi:10.1029/2007JG000674,
608 2008.

609



- 610 Aitkenhead, J.A., and McDowell, W.H.: Soil C:N ratio as a predictor of annual riverine DOC
611 flux at local and global scales, *Global Biogeochem. Cycles*, 14(1), 127–138,
612 doi:10.1029/1999GB900083, 2000.
613
- 614 Alaback, P.B.: Biodiversity patterns in relation to climate: The coastal temperate rainforests of
615 North America, *Ecol. Stud.*, 116, 105–133, doi:10.1007/978-1-4612-3970-3_7, 1996.
616
- 617 Algesten, G., Sobek, S., Bergström, A., Ågren, A., Tranvik, L. and Jansson, M.: Role of lakes for
618 organic carbon cycling in the boreal zone, *Global Change Biol.*, 10(1), 141–147,
619 doi:10.1111/j.1365-2486.2003.00721.x, 2004.
620
- 621 Alvarez-Cobelas, M., Angeler, D., Sánchez-Carrillo, S. and Almendros, G.: A worldwide view
622 of organic carbon export from catchments, *Biogeochemistry*, 107(1-3), 275–293,
623 doi:10.1007/s10533-010-9553-z, 2012.
624
- 625 Amon, R.M.W., and Benner, R.: Bacterial utilization of different size classes of dissolved
626 organic matter, *Limnol. Oceanogr.*, 41, 41–51, 1996.
627
- 628 Aufdenkampe, A., Mayorga, E., Raymond, P., Melack, J., Doney, S., Alin, S., Aalto, R., and
629 Yoo, K.: Riverine coupling of biogeochemical cycles between land, oceans, and atmosphere,
630 *Front. Ecol. Environ.*, 9(1), 53–60, doi:10.1890/100014, 2011.
631
- 632 Banner, A., LePage, P., Moran, J., and de Groot, A. (Eds.): The HyP3 Project: pattern,
633 process, and productivity in hypermaritime forests of coastal British Columbia -
634 a synthesis of 7-year results, Special Report 10, Res. Br., British Columbia Ministry Forests,
635 Victoria, British Columbia, 142 pp., available at:
636 <http://www.for.gov.bc.ca/hfd/pubs/Docs/Srs/Srs10.htm>, 2005.
637
- 638 Baum, A., Rixen, T. and Samiaji, J.: Relevance of peat draining rivers in central Sumatra for the
639 riverine input of dissolved organic carbon into the ocean, *Estuar. Coast Shelf Sci.*, 73, 563–570,
640 doi:10.1016/j.ecss.2007.02.012, 2007.
641
- 642 Berggren, M., Laudon, H., Haei, M., Ström, L., and Jansson, M.: Efficient aquatic bacterial
643 metabolism of dissolved low-molecular-weight compounds from terrestrial sources, *ISME J.*,
644 doi:10.1038/ismej.2009.120, 2010.
645
- 646 Bergström, A.K., and Jansson, M.: Bacterioplankton production in humic Lake Örträsket in
647 relation to input of bacterial cells and input of allochthonous organic carbon, *Microb. Ecol.*,
648 doi:10.1007/s002480000007, 2000.
649
- 650 Borcard, D., Gillet, F., and Legendre, P.: Numerical ecology with R, Springer, New York,
651 United States, doi:10.1007/978-1-4419-7976-6, 2011.
652
- 653 Borken, W., Ahrens, B., Schultz, C. and Zimmermann, L.: Site-to-site variability and temporal
654 trends of DOC concentrations and fluxes in temperate forest soils, *Global Change Biol.*, 17:
655 2428–2443, doi:10.1111/j.1365-2486.2011.02390.x, 2011.



- 656
657 Borges, A.V., Darchambeau, F., Teodoru, C.R., Marwick, T.R., Tamoooh, F., Geeraert, N.,
658 Omengo, F.O., Guérin, F., Lambert, T., Morana, C., Okuku, E., and Bouillon, S.: Globally
659 significant greenhouse-gas emissions from African inland waters, *Nature Geosci.*, 8, 637–642,
660 doi:10.1038/ngeo2486, 2015.
661
- 662 Liaw, A., and Wiener, M.: Classification and Regression by randomForest, *R News*, 2(3), 18–22,
663 2002.
664
- 665 Cole, J., Prairie, Y., Caraco, N., McDowell, W., Tranvik, L., Striegl, R., Duarte, C., Kortelainen,
666 P., Downing, J., Middelburg, J. and Melack, J.: Plumbing the Global Carbon Cycle: Integrating
667 Inland Waters into the Terrestrial Carbon Budget, *Ecosystems*, 10(1), 172–185,
668 doi:10.1007/s10021-006-9013-8, 2007.
669
- 670 International Union of Soil Sciences (IUSS) Working Group: World Reference Base for Soil
671 Resources, International soil classification system for naming soils and creating legends for soil
672 maps, World Soil Resources Reports No. 106, Food and Agricultural Organization of the United
673 Nations, Rome, Italy, 2015.
674
- 675 ISO Standard 9196: Liquid flow measurement in open channels - Flow measurements under ice
676 conditions, International Organization for Standardization, available online at www.iso.org,
677 1992.
678
- 679 ISO Standard 748: Hydrometry - Measurement of liquid flow in open channels using current-
680 meters or floats, International Organization for Standardization, available online at www.iso.org,
681 2007.
682
- 683 Cory, R.M., and McKnight, D.M.: Fluorescence spectroscopy reveals ubiquitous presence of
684 oxidized and reduced quinines in dissolved organic matter, *Environ. Sci. Technol.*, 39, 8142 -
685 8149, doi:10.1021/es0506962, 2005.
686
- 687 D'Amore, D.V., Edwards, R.T., and Biles, F.E.: Biophysical controls on dissolved organic
688 carbon concentrations of Alaskan coastal temperate rainforest streams, *Aquat. Sci.*,
689 doi:10.1007/s00027-015-0441-4, 2015a.
690
- 691 D'Amore, D.V., Edwards, R.T., Herendeen, P.A., Hood, E., and Fellman, J.B.: Dissolved
692 organic carbon fluxes from hydrogeologic units in Alaskan coastal temperate rainforest
693 watersheds, *Soil Sci. Soc. Am. J.*, 79:378–388, doi:10.2136/sssaj2014.09.0380, 2015b.
694
- 695 D'Amore, D.V., Biles, F.E., Nay, M., Rupp, T.S.: Watershed carbon budgets in the southeastern
696 Alaskan coastal forest region, in: *Baseline and projected future carbon storage and greenhouse-
697 gas fluxes in ecosystems of Alaska*, U.S. Geological Survey Professional Paper, 1826, 196 p.,
698 2016.
699
- 700 DellaSala, D.A.: *Temperate and Boreal Rainforests of the World*, Island Press, Washington,
701 D.C., 2011.



- 702
703 Eaton, B., and Moore, R.D.: Regional hydrology, in Compendium of forest hydrology and
704 geomorphology in British Columbia, Land Management Handbook 66, Pike, R.G., Redding,
705 T.E., Moore, R.D., Winker, R.D., and Bladon, K.D. (Eds.), British Columbia Ministry Forests,
706 Victoria, British Columbia, and FORREX Forum for Research and Extension in Natural
707 Resources, Kamloops, British Columbia, available at:
708 www.for.gov.bc.ca/hfd/pubs/Docs/Lmh/Lmh66.htm, 2010.
709
- 710 Emili, L. and Price, J.: Biogeochemical processes in the soil-groundwater system of a forest-
711 peatland complex, north coast British Columbia, Canada, *Northwest Sci.*, 88, 326–348,
712 doi:10.3955/046.087.0406, 2013.
713
- 714 Fasching, C., Behounek, B., Singer, G. and Battin, T.: Microbial degradation of terrigenous
715 dissolved organic matter and potential consequences for carbon cycling in brown-water streams,
716 *Sci. Rep.*, 4, 4981, doi:10.1038/srep04981, 2014.
717
- 718 Fellman, J., Hood, E., D’Amore, D., Edwards, R. and White, D.: Seasonal changes in the
719 chemical quality and biodegradability of dissolved organic matter exported from soils to streams
720 in coastal temperate rainforest watersheds, *Biogeochemistry*, 95, 277–293, doi:10.1007/s10533-
721 009-9336-6, 2009a.
722
- 723 Fellman, J., Hood, E., Edwards, R. and D’Amore, D.: Changes in the concentration,
724 biodegradability, and fluorescent properties of dissolved organic matter during stormflows in
725 coastal temperate watersheds, *J. Geophys. Res. Biogeosci.*, 114, doi:10.1029/2008JG000790,
726 2009b.
727
- 728 Fellman, J., Hood, E. and Spencer, R.: Fluorescence spectroscopy opens new windows into
729 dissolved organic matter dynamics in freshwater ecosystems: A review, *Limnol. Oceanogr.*, 55,
730 24522462, doi:10.4319/lo.2010.55.6.2452, 2010.
731
- 732 Finlay, J.C., and Kendall, C.: Stable isotope tracing of temporal and spatial variability in organic
733 matter sources and variability in organic matter sources to freshwater ecosystems, in *Stable*
734 *Isotopes in Ecology and Environmental Science*, 2, Michener, R., and Lajtha, K. (Eds),
735 Blackwell Publishing Ltd, Oxford, UK, 283-324, 2007.
736
- 737 Fitzgerald, D., Price, J., and Gibson, J.: Hillslope-swamp interactions and flow pathways in a
738 hypermaritime rainforest, British Columbia, *Hydrol. Process.*, 17, 3005-3022,
739 doi:10.1002/hyp.1279, 2003.
740
- 741 Gibson, J.J., Price, J.S., Aravena, R., Fitzgerald, D.F., and Maloney, D.: Runoff generation in a
742 hypermaritime bog-forest upland, *Hydrol. Process*, 14, 2711-2730, doi: 10.1002/1099-
743 1085(20001030)14:15<2711::AID-HYP88>3.0.CO;2-2, 2000.
744
- 745 Glatzel, S., Kalbitz, K., Dalva, M., and Moore, T.: Dissolved organic matter properties and their
746 relationship to carbon dioxide efflux from restored peat bogs, *Geoderma*, 113, 397-411, 2003.
747



- 748 Gonzalez Arriola S., Frazer, G.W., Giesbrecht, I.: LiDAR-derived watersheds and their metrics
749 for Calvert Island, Hakai Institute, doi:dx.doi.org/10.21966/1.15311, 2015.
750
- 751 Gorham, E., Lehman, C., Dyke, A., Clymo, D., and Janssens, J.: Long-term carbon sequestration
752 in North American peatlands, *Quat. Sci. Review*, 58, 77-82, 2012.
753
- 754 Graeber, D., Gelbrecht, J., Pusch, M., Anlanger, C. and von Schiller, D.: Agriculture has
755 changed the amount and composition of dissolved organic matter in Central European headwater
756 streams, *Sci. Total Environ.*, 438, 435–446, doi:10.1016/j.scitotenv.2012.08.087, 2012.
757
- 758 Green, R.N.: Reconnaissance level terrestrial ecosystem mapping of priority landscape units of
759 the coast EBM planning area: Phase 3, Prepared for British Columbia Ministry Forests, Lands
760 and Natural Resource Ops., Blackwell and Associates, Vancouver, Canada, 2014.
761
- 762 Guillemette, F. and Giorgio, P.: Reconstructing the various facets of dissolved organic carbon
763 bioavailability in freshwater ecosystems, *Limnol. Oceanogr.*, 56, 734–748,
764 doi:10.4319/lo.2011.56.2.0734, 2011.
765
- 766 Harrison, J., Caraco, N. and Seitzinger, S.: Global patterns and sources of dissolved organic
767 matter export to the coastal zone: Results from a spatially explicit, global model, *Global
768 Biogeochem. Cycles*, 19, doi:10.1029/2005gb002480, 2005.
769
- 770 Hill, D.F., Bruhis, N., Calos, S.E., Arendt, A., and Beamer, J.: Spatial and temporal variability of
771 freshwater discharge into the Gulf of Alaska, *J. Geophys. Res. Oceans*, 120, 634-646,
772 doi:10.1002/2014JC010395, 2015.
773
- 774 Helms, J., Stubbins, A., Ritchie, J., Minor, E., Kieber, D. and Mopper, K.: Absorption spectral
775 slopes and slope ratios as indicators of molecular weight, source, and photobleaching of
776 chromophoric dissolved organic matter, *Limnol. Oceanogr.*, 53, 955–969,
777 doi:10.4319/lo.2008.53.3.0955, 2008.
778
- 779 Helton, A., Wright, M., Bernhardt, E., Poole, G., Cory, R. and Stanford, J.: Dissolved organic
780 carbon lability increases with water residence time in the alluvial aquifer of a river floodplain
781 ecosystem, *J. Geophys. Res. Biogeosciences*, 120, 693–706, doi:10.1002/2014JG002832, 2015.
782
- 783 Hoffman, K.M., Gavin, D.G., Lertzman, K.P., Smith, D.J., Starzomski, B.M.: 13,000 years of
784 fire history derived from soil charcoal in a British Columbia coastal temperate rain forest,
785 *Ecosphere*, 7, e01415, doi:10.1002/ecs2.1415, 2016.
786
- 787 Hudson, N., Baker, A. and Reynolds, D.: Fluorescence analysis of dissolved organic matter in
788 natural, waste and polluted waters-a review, *River Res. Appl.*, 23, 631–649,
789 doi:10.1002/rra.1005, 2007.
790
- 791 Johnson, M., Couto, E., Abdo, M. and Lehmann, J.: Fluorescence index as an indicator of
792 dissolved organic carbon quality in hydrologic flowpaths of forested tropical watersheds,
793 *Biogeochemistry*, 105, 149–157, doi:10.1007/s10533-011-9595-x, 2011.



- 794
795 Judd, K., Crump, B. and Kling, G.: Variation in dissolved organic matter controls bacterial
796 production and community composition, *Ecology*, 87, 2068–2079, doi:10.1890/0012-
797 9658(2006)87[2068:VIDOMC]2.0.CO;2, 2006.
798
799 Kaiser, K., Guggenberger, G., Haumaier, L., and Zech, W.: Dissolved organic matter sorption on
800 sub soils and minerals studied by ¹³C-NMR and DRIFT spectroscopy, *Eur. J. Soil. Sci.*, 48, 301-
801 310, doi:10.1111/j.1365-2389.1997.tb00550.x, 1997.
802
803 Kalbitz, K., Schwesig, D., Rethemeyer, J., and Matzner, E.: Stabilization of dissolved organic
804 matter by sorption to the mineral soil, *Soil Biol. Biogeochem.*, 37, 1319-1331, doi:
805 10.1016/j.soilbio.2004.11.028, 2005.
806
807 Kalbitz, K., Schmerwitz, J., Schwesig, D. and Matzner, E.: Biodegradation of soil-derived
808 dissolved organic matter as related to its properties, *Geoderma*, 113, 273–291,
809 doi:10.1016/S0016-7061(02)00365-8, 2003.
810
811 Kling, G., Kipphut, G., Miller, M. and O'Brien, W.: Integration of lakes and streams in a
812 landscape perspective: the importance of material processing on spatial patterns and temporal
813 coherence, *Freshwater Biol.*, 43, 477–497, doi:10.1046/j.1365-2427.2000.00515.x, 2000.
814
815 Koehler, A.-K., Murphy, K., Kiely, G. and Sottocornola, M.: Seasonal variation of DOC
816 concentration and annual loss of DOC from an Atlantic blanket bog in South Western Ireland,
817 *Biogeochemistry*, 95, 231–242, doi:10.1007/s10533-009-9333-9, 2009.
818
819 Lakowicz, J.R.: *Principles of Fluorescence Spectroscopy*, 2, Kluwer Academic, New York,
820 1999.
821
822 Kritzberg, ES, Cole, JJ and Pace, ML: Autochthonous versus allochthonous carbon sources of
823 bacteria: Results from whole-lake ¹³C addition experiments, *Limnol. Oceanogr.*, 49, 588-596,
824 doi:10.4319/lo.2004.49.2.0588, 2004.
825
826 Lalonde, K., Middlestead, P., Gélinas, Y.: Automation of ¹³C/¹²C ratio measurement for
827 freshwater and seawater DOC using high temperature combustion, *Limnol. Oceanogr. Methods*,
828 12, 816-829, doi:10.4319/lom.2014.12.816, 2014.
829
830 Leach, J., Larsson, A., Wallin, M., Nilsson, M. and Laudon, H.: Twelve year interannual and
831 seasonal variability of stream carbon export from a boreal peatland catchment, *J. Geophys. Res.*
832 121, 1851–1866, doi:10.1002/2016JG003357, 2016.
833
834 Legendre, P., and Durand, S.: rdaTest, Canonical redundancy analysis, R package version 1.11,
835 available at <http://adn.biol.umontreal.ca/~numerica/ecology/Rcode/>, 2014.
836



- 837 Lepistö, A., Futter, M.N. and Kortelainen, P.: Almost 50 years of monitoring shows that climate,
838 not forestry, controls long-term organic carbon fluxes in a large boreal watershed, *Glob. Change*
839 *Biol.*, 20, 1225–1237, doi:10.1111/gcb.12491, 2014.
840
- 841 Lorenz, D., Runkel, R., and De Cicco, L.: rloadest, River Load Estimation, R package version
842 0.4.2, available at <https://github.com/USGS-R/rloadest>, 2015.
843
- 844 Ludwig, W., Probst, J. and Kempe, S.: Predicting the oceanic input of organic carbon by
845 continental erosion, *Global Biogeochem. Cycles*, 10, 23–41, doi:10.1029/95GB02925, 1996.
846
- 847 Marschner, B., and Kalbitz, K.: Controls on bioavailability and biodegradability of dissolved
848 organic matter in soils, *Geoderma*, 113, 211–235, 2003.
849
- 850 Mayorga, E., Seitzinger, S., Harrison, J., Dumont, E., Beusen, A., Bouwman, A.F., Fekete, B.,
851 Kroeze, C. and Dreht, G.: Global Nutrient Export from WaterSheds 2 (NEWS 2): Model
852 development and implementation, *Environ. Model. Softw.*, 25, 837–853,
853 doi:10.1016/j.envsoft.2010.01.007, 2010.
854
- 855 McCallister, L. S. and Giorgio, P. A.: Direct measurement of the $\delta^{13}\text{C}$ signature of carbon
856 respired by bacteria in lakes: Linkages to potential carbon sources, ecosystem baseline
857 metabolism, and CO_2 fluxes, *Limnol. Oceanogr.*, 53, 1204, doi:10.4319/lo.2008.53.4.1204,
858 2008.
859
- 860 McClelland, J., Townsend-Small, A., Holmes, R., Pan, F., Stieglitz, M., Khosh, M. and Peterson,
861 B.: River export of nutrients and organic matter from the North Slope of Alaska to the Beaufort
862 Sea, *Water Resour. Res.*, 50, 1823–1839, doi:10.1002/2013WR014722, 2014.
863
- 864 McKnight, D., Boyer, E., Westerhoff, P., Doran, P., Kulbe, T. and Andersen, D.:
865 Spectrofluorometric characterization of dissolved organic matter for indication of precursor
866 organic material and aromaticity, *Limnol. Oceanogr.*, 46, 38–48, doi:10.4319/lo.2001.46.1.0038,
867 2001.
868
- 869 McLaren, D., Fedje, D., Hay, M.B., Mackie, Q., Walker, I.J., Shugar, D.H., Eamer, J.B.R., Lian,
870 O.B., and Neudorf, C.: A post-glacial sea level hinge on the central Pacific coast of Canada,
871 *Quat. Sci. Review.*, 97, 148-169, 2014.
872
- 873 Meybeck, M.: Carbon, nitrogen, and phosphorus transport by world rivers, *Am. J. Sci.*, 282, 401-
874 450, Available from: <http://earth.geology.yale.edu/~ajs/1982/04.1982.01.Maybeck.pdf>, 1982.
875
- 876 Moore, R.D.: Introduction to salt dilution gauging for streamflow measurement part III: Slug
877 injection using salt in solution, *Streamline Watershed Management Bulletin*, 8(2), 1-6, 2005.
878
- 879 Moreira-Turcq, P., Seyler, P., Guyot, J. and Etcheber, H.: Exportation of organic carbon from the
880 Amazon River and its main tributaries, *Hydrol. Process.*, 17, 1329–1344, doi:10.1002/hyp.1287,
881 2003.



- 882
883 Mulholland, P. and Watts, J.: Transport of organic carbon to the oceans by rivers of North
884 America: a synthesis of existing data, *Tellus*, 34, 176–186, doi:10.1111/j.2153-
885 3490.1982.tb01805.x, 1982.
886
887 Murphy, K., Stedmon, C., Graeber, D. and Bro, R.: Fluorescence spectroscopy and multi-way
888 techniques. *PARAFAC, Anal. Methods*, 5, 6557–6566, doi:10.1039/C3AY41160E, 2013.
889
890 Murphy K., Stedmon, C., Wenig, P., Bro, R.: OpenFluor- A spectral database of auto-
891 fluorescence by organic compounds in the environment, *Anal. Methods*, 6, 658-661,
892 DOI:10.1039/C3AY41935E, 2014.
893
894 Olefeldt, D., Roulet, N., Giesler, R. and Persson, A.: Total waterborne carbon export and DOC
895 composition from ten nested subarctic peatland catchments- importance of peatland cover,
896 groundwater influence, and inter-annual variability of precipitation patterns, *Hydrol. Process.*,
897 27, 2280-2294, doi:10.1002/hyp.9358, 2013.
898
899 Poulin, B., Ryan, J. and Aiken, G.: Effects of iron on optical properties of dissolved organic
900 matter, *Environ. Sci. Technol.*, 48, 10098–106, doi:10.1021/es502670r, 2014.
901
902 R Core Team, R: A language and environment for statistical computing, R Foundation for
903 Statistical Computing, Vienna, Austria, <http://www.R-project.org/>, 2013.
904
905 Raymond, P., Saiers, J. and Sobczak, W.: Hydrological and biogeochemical controls on
906 watershed dissolved organic matter transport: pulse-shunt concept, *Ecology*, 97, 5-16,
907 doi:10.1890/14-1684.1, 2016.
908
909 Regnier, P., Friedlingstein, P., Ciais, P., Mackenzie, F., Gruber, N., Janssens, I., Laruelle, G.,
910 Lauerwald, R., Luyssaert, S., Andersson, A., Arndt, S., Arnosti, C., Borges, A., Dale, A.,
911 Gallego-Sala, A., Godd ris, Y., Goossens, N., Hartmann, J., Heinze, C., Ilyina, T., Joos, F.,
912 LaRowe, D., Leifeld, J., Meysman, F., Munhoven, G., Raymond, P., Spahni, R., Suntharalingam,
913 P. and Thullner, M.: Anthropogenic perturbation of the carbon fluxes from land to ocean, *Nat.*
914 *Geosci.*, 6, 597–607, doi:10.1038/ngeo1830, 2013.
915
916 Roddick, J.R.: *Geology, Rivers Inlet-Queens Sound, British Columbia, Open File 3278,*
917 *Geological Survey of Canada, Ottawa, Canada, 1996.*
918
919 Royer, T.C., Coastal fresh water discharge in the northeast, Pacific, *J. Geophys. Res.*, 87, 2017-
920 2021, 1982.
921
922 Runkel, R.L., Crawford, C.G., and Cohn, T.A.: Load Estimator (LOADEST): A FORTRAN
923 program for estimating constituent loads in streams and rivers, U.S. Geological Survey
924 *Techniques and Methods Book 4, Chapter A5, 65 pp.*, 2004.
925



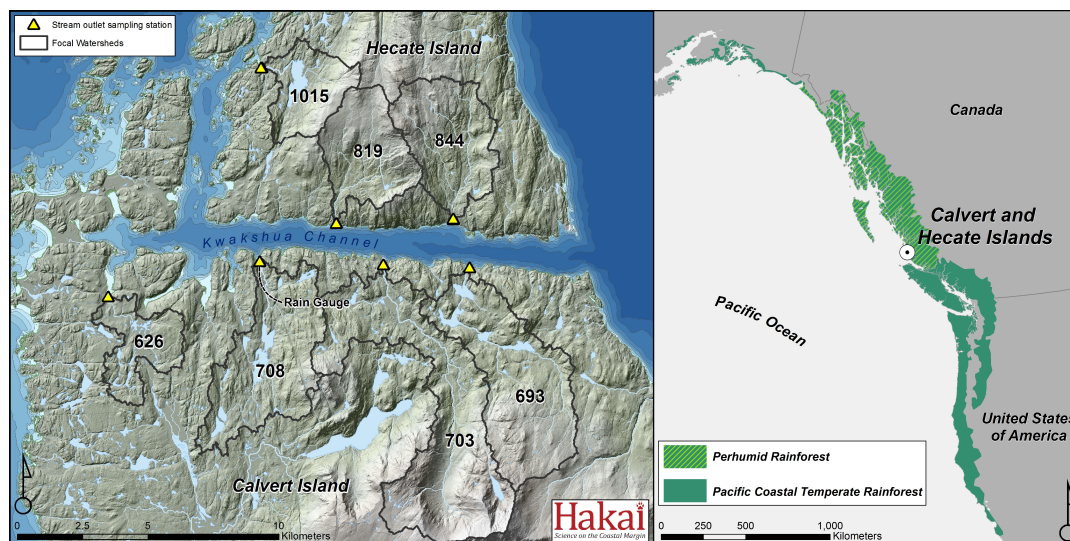
- 926 Spencer, R., Butler, K. and Aiken, G.: Dissolved organic carbon and chromophoric dissolved
927 organic matter properties of rivers in the USA, *J. Geophys. Res. Biogeosciences*, 117(G03001),
928 doi:10.1029/2011JG001928, 2012.
929
- 930 Spencer, R.G, Hernes, P.J., Dinga, B., Wabakanghanzi, J., Drake, T. and Six, J.: Origins,
931 seasonality, and fluxes of organic matter in the Congo River, *Global Biogeochem. Cycles*, 30,
932 1105–1121, doi:10.1002/2016GB005427, 2016.
933
- 934 Spencer, R.G., Hernes, P.J, Ruf, R., Baker, A., Dyda, R.Y., Stubbins, A., and Six, J.: Temporal
935 controls on dissolved organic matter and lignin biogeochemistry in a pristine tropical river,
936 Democratic Republic of Congo, *J. Geophys. Res.*, 115, G03013, doi:10.1029/2009JG001180,
937 2010.
938
- 939 Stackpoole, S., Butman, D., Clow, D., Verdin, K, Gaglioti, B., and Striegl, R.: Carbon burial,
940 transport, and emission from inland aquatic ecosystems in Alaska, in: *Baseline and projected
941 future carbon storage and greenhouse-gas fluxes in ecosystems of Alaska*, Zhiliang, Z., and
942 David, A. (Eds.), U.S. Geological Survey Professional Paper, 1826, 196 p., 2016.
943
- 944 Stedmon, C. and Bro, R.: Characterizing dissolved organic matter fluorescence with parallel
945 factor analysis: a tutorial, *Limnol. Oceanogr. Methods*, 6, 572–579,
946 doi:10.4319/lom.2008.6.572b, 2008.
947
- 948 Stedmon, C., Markager, S., Bro, R., Stedmon, C., Markager, S. and Bro, R.: Tracing dissolved
949 organic matter in aquatic environments using a new approach to fluorescence spectroscopy, *Mar.
950 Chem.*, doi:10.1016/S0304-4203(03)00072-0, 2003.
951
- 952 Stevenson, F.J.: *Humus Chemistry: Genesis, Composition, Reactions*, 2, Jon Wiley and Sons
953 Inc., New York, United States of America, 1994.
954
- 955 Tank, S., Raymond, P., Striegl, R., McClelland, J., Holmes, R., Fiske, G. and Peterson, B.: A
956 land-to-ocean perspective on the magnitude, source and implication of DIC flux from major
957 Arctic rivers to the Arctic Ocean, *Global Biogeochem. Cycles*, 26, GB4018,
958 doi:10.1029/2011GB004192, 2012.
959
- 960 Thompson, S.D., Nelson, T.A., Giesbrecht, I., Frazer, G., and Saunders, S.C.: Data-driven
961 regionalization of forested and non-forested ecosystems in coastal British Columbia with LiDAR
962 and RapidEye imagery, *Appl. Geogr.*, 69, 35–50, doi: 10.1016/j.apgeog.2016.02.002,
963 2016.
964
- 965 Trant, A.J., Nijjland, W., Hoffman, K.M., Mathews, D.L., McLaren, D., Nelson, T.A.,
966 Starzomski, B.M.: Intertidal resource use over millennia enhances forest productivity, *Nature
967 Commun.*, 7, 12491, doi: 10.1038/ncomms12491, 2016.
968



- 969 van Hees, P., Jones, D., Finlay, R., Godbold, D. and Lundström, U.: The carbon we do not see-
970 the impact of low molecular weight compounds on carbon dynamics and respiration in forest
971 soils: a review, *Soil Biol. Biochem.*, 37, 1–13, doi:10.1016/j.soilbio.2004.06.010, 2005.
972
- 973 Wallin, M., Weyhenmeyer, G., Bastviken, D., Chmiel, H., Peter, S., Sobek, S. and Klemetsson,
974 L.: Temporal control on concentration, character, and export of dissolved organic carbon in two
975 hemiboreal headwater streams draining contrasting catchments, *J. Geophys. Res. Biogeosci.* 120,
976 832–846, doi:10.1002/2014jg002814, 2015.
977
- 978 Wang, T., Hamann, A., Spittlehouse, D.L., and Murdock, T.Q.: ClimateWNA- High resolution
979 spatial climate data for Western North America, *J. Appl. Meteorol. Climatol.*, 51, 16-29,
980 doi:dx.doi.org/10.1175/JAMC-D-11-043.1, 2012.
981
- 982 Waterloo, M., Oliveira, S., Drucker, D., Nobre, A., Cuartas, L., Hodnett, M., Langedijk, I., Jans,
983 W., Tomasella, J., Araújo, A., Pimentel, T. and Estrada, J.: Export of organic carbon in run-off
984 from an Amazonian rainforest blackwater catchment, *Hydrol. Process.*, 20, 2581–2597,
985 doi:10.1002/hyp.6217, 2006.
986
- 987 Weishaar, J.L., Aiken, G.R., Bergamaschi, B.A., Fram, M.S., Fujii, R. and Mopper, K.:
988 Evaluation of specific ultraviolet absorbance as an indicator of the chemical composition and
989 reactivity of dissolved organic carbon, *Environ. Sci. Technol.*, 37, 4702–8,
990 doi:10.1021/es030360x, 2003.
991
- 992 Wickland, K., Neff, J., and Aiken, G.: Dissolved Organic Carbon in Alaskan Boreal Forest:
993 Sources, Chemical Characteristics, and Biodegradability, *Ecosystems*, 10, 1323-1340, 2007.
994
- 995 Wilson, H.F. and Xenopoulos, M.A.: Effects of agricultural land use on the composition of
996 fluvial dissolved organic matter, *Nat. Geosci.*, 2, 37–41, doi:10.1038/ngeo391, 2009.
997
- 998 Wolf, E.C., Mitchell, A.P., and Schoonmaker, P.K.: *The Rain Forests of Home: An Atlas of*
999 *People and Place*, Ecotrust, Pacific GIS, Inforain, and Conservation International, Portland,
1000 Oregon, 24 pp., available at: http://www.inforain.org/pdfs/ctrf_atlas_orig.pdf, 1995.
1001
- 1002 Worrall, F., Burt, T., and Adamson, J.: Can climate change explain increases in DOC flux from
1003 upland peat catchments?, *Sci. Total. Environ.*, 326, 95–112,
1004 doi:10.1016/j.scitotenv.2003.11.022, 2004.
1005
- 1006 Yamashita, Y. and Jaffé, R.: Characterizing the Interactions between Trace Metals and Dissolved
1007 Organic Matter Using Excitation–Emission Matrix and Parallel Factor Analysis, *Environ. Sci.*
1008 *Technol.*, 42, 7374–7379, doi:10.1021/es801357h, 2008.
1009
- 1010 Yamashita, Y., Kloeppel, B., Knoepp, J., Zausen, G. and Jaffé, R.: Effects of Watershed History
1011 on Dissolved Organic Matter Characteristics in Headwater Streams, *Ecosystems*, 14, 1110–1122,
1012 doi:10.1007/s10021-011-9469-z, 2011.



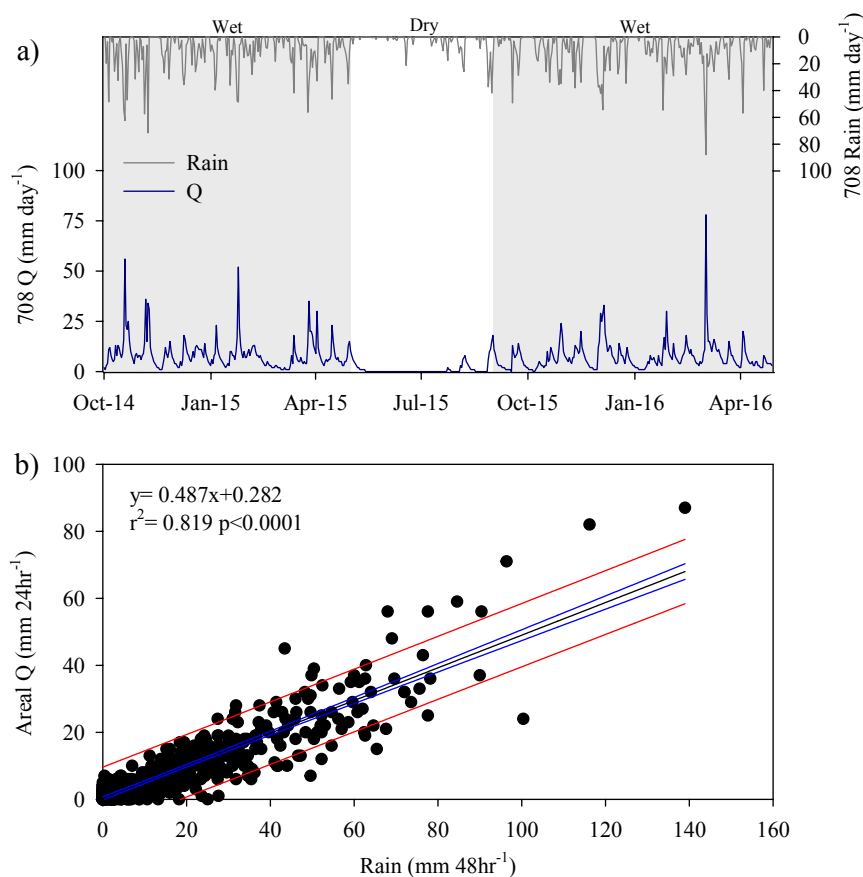
1013 **Figure 1.** The location of Calvert Island, British Columbia, within the perhumid region of the
1014 Pacific coastal temperate rainforest (right) and the study area on Calvert and Hecate Islands,
1015 including the seven study watersheds, corresponding stream outlet sampling stations, and
1016 location of the rain gauge (left). Characteristics of individual watersheds are described in Table
1017 1.
1018



1019
1020
1021
1022
1023
1024
1025
1026
1027
1028
1029
1030
1031
1032
1033
1034
1035
1036
1037
1038
1039
1040



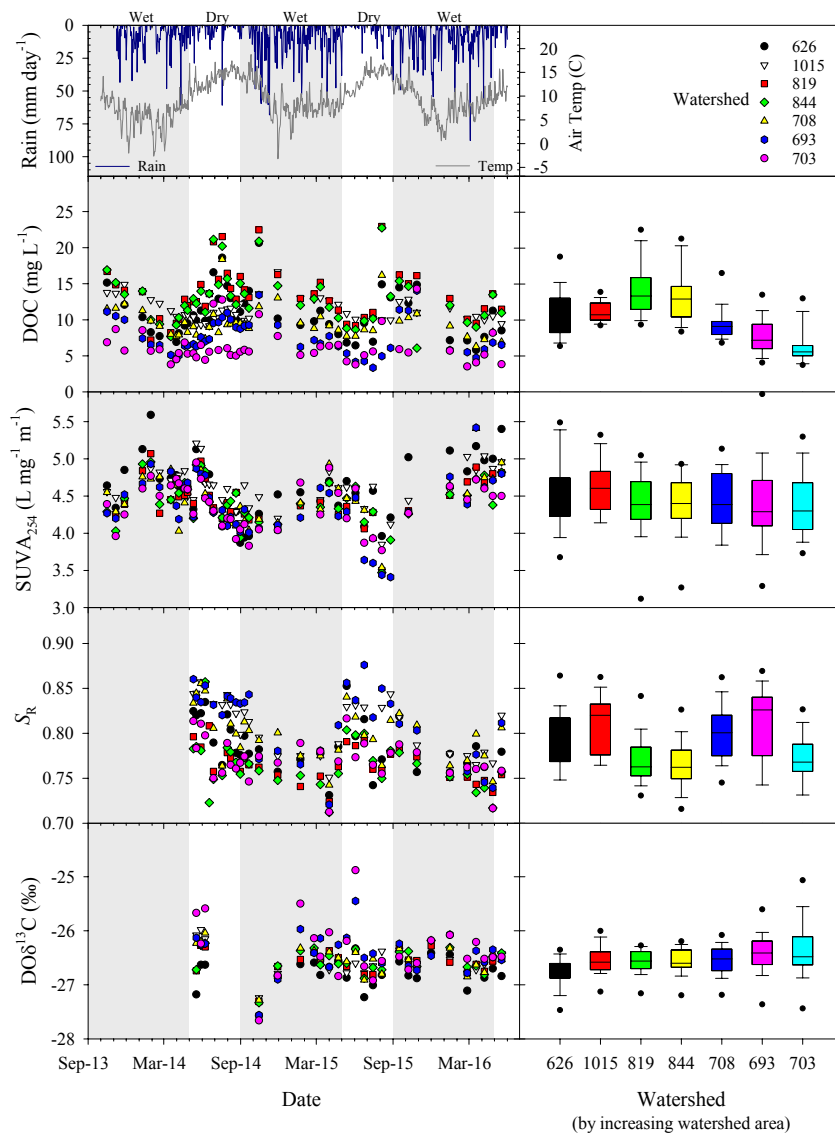
1041 **Figure 2.** Hydrological patterns reflect the high amounts of precipitation and rapid runoff
 1042 response typical of watersheds located in the study area (a) the hydrograph and precipitation
 1043 record from Watershed 708 illustrates seasonal patterns in runoff and rainfall for the study period
 1044 of October 1, 2015-April 30, 2016. Grey shading indicates the wet period (September 1-April
 1045 30) and the unshaded region indicates the dry period (May 1-August 30) (b) Correlation of daily
 1046 (24 hour) areal runoff (discharge of all watersheds combined) to 48 hour total rainfall recorded at
 1047 watershed 708. For the period of study, comparisons of daily runoff to 48-hr rainfall
 1048 (runoff:rainfall mean= 0.92, std \pm 0.27) indicated that the response in discharge from catchments
 1049 is relatively rapid following precipitation.



1050
 1051

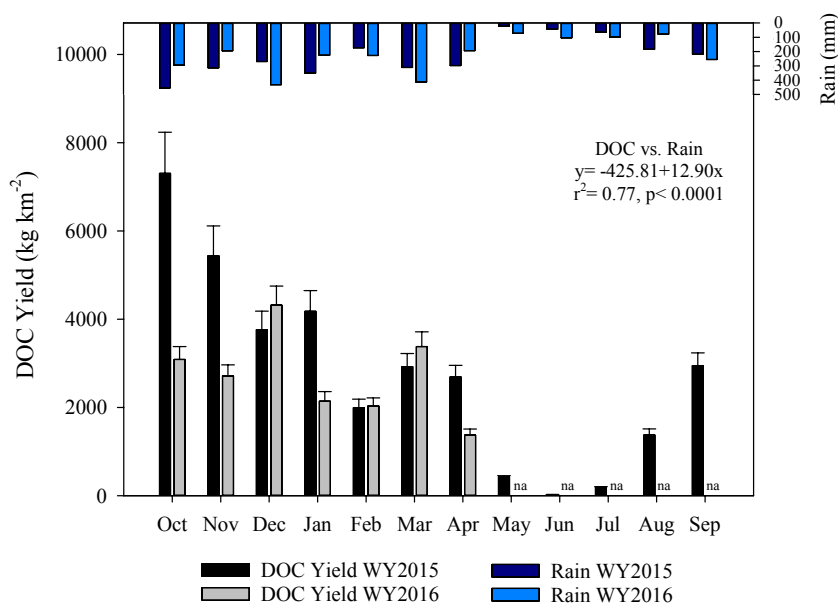


1052 **Figure 3.** Seasonal (timelines, by date) and spatial (boxplots, by watershed) patterns in DOC
 1053 concentration and DOM composition for stream water collected at the outlets of the seven study
 1054 watersheds on Calvert and Hecate Islands. Daily precipitation and annual temperature are shown
 1055 in the top left panel. Grey shading indicates the wet period (September 1-April 30) and the
 1056 unshaded region indicates the dry period of each water year.
 1057





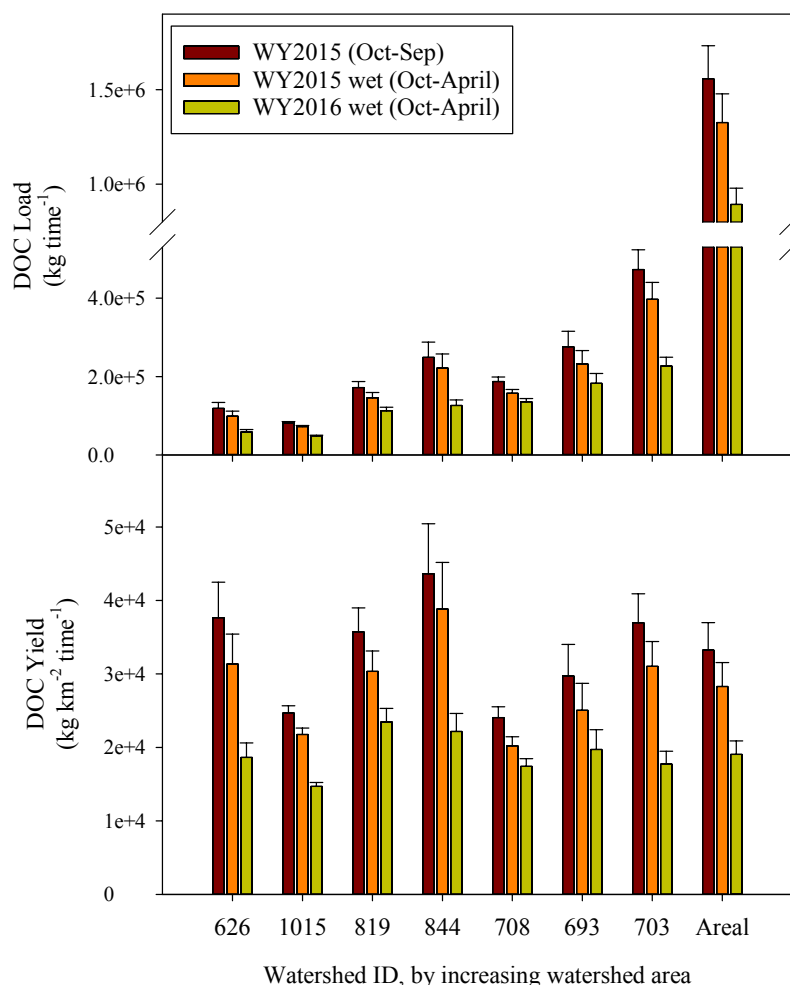
1059 **Figure 4.** Monthly areal DOC yields and precipitation for water year 2015 (WY2015) and the
 1060 wet period (October 1-April 30) of water year 2016 (WY2016). Error bars represent standard
 1061 error. Total rain and DOC yield were significantly correlated ($r^2 = 0.77$) and months of higher
 1062 rain produced higher DOC yields. In WY2015, the majority of DOC export (~94% of annual
 1063 load) occurred during the wet period (~88% of annual precipitation).



1064
 1065
 1066
 1067
 1068
 1069
 1070
 1071
 1072
 1073
 1074
 1075
 1076
 1077
 1078
 1079
 1080
 1081

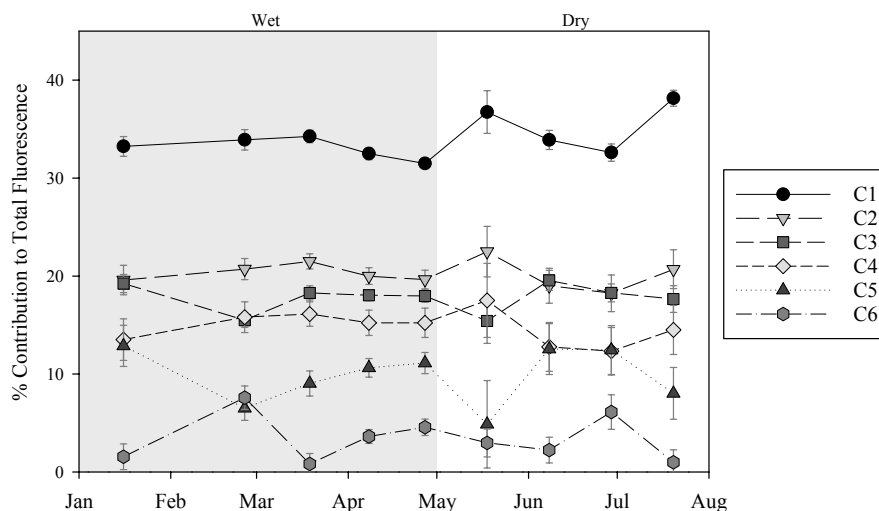


1082 **Figure 5:** DOC loads and yields for the seven study watersheds and the total area of study (all
 1083 watersheds combined, or “areal”) on Calvert and Hecate Islands for the complete water year
 1084 2015 (WY2015; Oct 1 - Sep 30), and October 1- April 30 of the wet period for water year 2015
 1085 (WY2015 wet) and water year 2016 (WY2016 wet). Because DOC yields were only available
 1086 for September in WY2015, this month was excluded from the wet period totals in order to make
 1087 similar comparisons between years. Error bars represent standard error. Total DOC load tended
 1088 to increase by increasing watershed area, and the total amount of DOC exported during the wet
 1089 period was higher in WY2015 compared to WY2016. DOC yield was also higher for the wet
 1090 period of WY2015 compared to WY2016, but differences between watersheds were independent
 1091 of total watershed area, indicated different drivers of DOC export on a per-area basis.





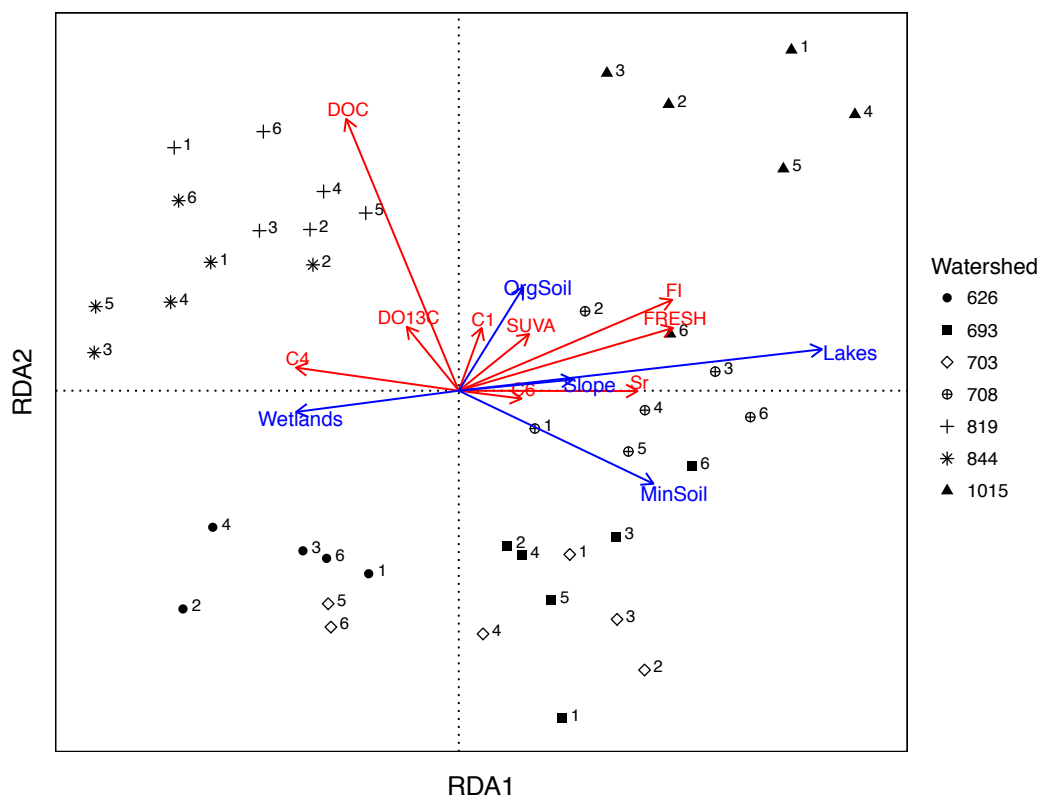
1093 **Figure 6:** Percent contribution of the six components identified in parallel factor analysis
 1094 (PARAFAC) for samples collected every three weeks from January-July, 2016 from the seven
 1095 study watersheds on Calvert and Hecate Islands study watersheds. Points represent means \pm
 1096 standard deviation for all watersheds combined. The grey shading indicates the wet period and
 1097 the unshaded region indicates the dry period.



1098
 1099
 1100
 1101
 1102
 1103
 1104
 1105
 1106
 1107
 1108
 1109
 1110
 1111
 1112
 1113
 1114
 1115
 1116
 1117
 1118
 1119



1120 **Figure 7:** Results from the partial-Redundancy analysis (RDA; type 2 scaling) of DOC
 1121 concentration and DOM composition versus watershed characteristics. Angles between vectors
 1122 represent correlation, i.e., smaller angles indicate higher correlation. Symbols represent different
 1123 watersheds, and numbers on symbols represent the sample month in 2016: 1= January, 2=
 1124 February, 3= March, 4= early April, 5= late April, and 6= May.
 1125



1126



1127 **Table 1:** Watershed characteristics, discharge, DOC concentrations, and DOC yields for the seven study watersheds on Calvert and
 1128 Hecate Islands. Additional details on the methods used to determine watershed characteristics can be found in Supplementary
 1129 Material.

Water- shed	Area (km ²)	Avg. Slope (%)	Lakes (% Area)	Wetlands (%Area)	Avg. Depth Organic Soils (cm)	Avg. Depth Mineral Soils (cm)	Total Q Yield* (mm)	DOC ^a (mg L ⁻¹)	Q- weighted Avg. DOC* (mg L ⁻¹)	DOC Annual Yield ^b WY2015* (Mg C km ⁻²)	DOC Monthly Yield ^b Wet Season** (Mg C km ⁻²)	DOC Monthly Yield ^b Dry Season*** (Mg C km ⁻²)
626	3.2	21.7	4.7	48.0	39.4 ±24.3	30.8 ±8.3	3673	11.0 ±3.5	15.3	37.7 (31.9 – 44.2)	3.59 (3.05 – 4.18)	0.62 (0.49 – 0.77)
1015	3.3	34.2	9.1	23.8	39.5 ±17.2	33.7 ±8.6	3052	11.2 ±1.6	12.9	24.7 (23.6 – 25.8)	2.56 (2.45 – 2.78)	0.27 (0.25 – 0.28)
819	4.8	30.1	0.3	50.2	37.9 ±19.1	29.8 ±5.7	3066	14.0 ±3.5	19.3	35.7 (31.7 – 40.2)	3.80 (3.37 – 5.10)	0.57 (0.48 – 0.67)
844	5.7	32.5	0.3	35.2	35.4 ±18.0	29.1 ±6.4	4129	13.1 ±3.6	15.9	43.6 (34.2 – 54.9)	4.24 (3.36 – 5.30)	0.54 (0.36 – 0.77)
708	7.8	28.5	7.5	46.3	36.2 ±19.7	29.9 ±6.0	3805	9.5 ±2.4	10.9	24.1 (22.2 – 26.0)	2.67 (2.46 – 4.07)	0.38 (0.34 – 0.43)
693	9.3	30.2	4.4	42.8	35.4 ±16.1	30.2 ±6.4	5866	7.7 ±2.5	8.4	29.7 (25.9 – 34.0)	3.19 (2.79 – 4.94)	0.41 (0.32 – 0.52)
703	12.8	40.3	1.9	24.3	37.3 ±16.5	35.8 ±13.4	6058	6.3 ±2.6	9.0	37.0 (32.5 – 42.0)	3.48 (3.07 – 4.02)	0.64 (0.52 – 0.77)
All	46.9	32.7	3.7	37.1	37.4 ±17.7	32.2 ±9.2	4730	10.4 ±3.8	11.1	33.3 (28.9 – 38.1)	3.35 (2.94 – 4.40)	0.50 (0.41 – 0.62)

* Calculated for water year 2015 (WY2015; Oct 1, 2014–Sep 30, 2015)

** Wet period average monthly yield calculated from October–April and September, WY2015 and October–April, WY2016

*** Dry period average monthly yield calculated from May–August, WY2015

^a Mean ± standard deviation

^b Total ± 95% confidence interval



1131 **Table 2:** Spectral composition for the six fluorescence components identified using PARAFAC, including excitation (Ex.) and
 1132 emission (Em.) peak values, percent composition across all samples, and likely structure and characteristics of the fluorescent
 1133 component based on previous studies.

Component	Ex. (nm)	Em. (nm)	% Composition ^a	Potential structure/ Characteristics	Previous studies with comparable results
C1	315	436	34.1 ±2.2 (31.1-39.3)	Humic-like, less processed terrestrial, low molecular weight, enriched fulvic acid	Coble, 2007; Garcia et al. 2015; Graeber et al. 2012; Walker et al. 2014; Yamashita et al. 2011.
C2	270/ 380	484	20.2 ±1.9 (16.1-25.6)	Not commonly reported, similarities to humic-like, more processed terrestrial, high molecular weight	Boehme & Coble, 2000; Coble et al. 1998; La Pierre et al. 2014; Stedmon et al. 2003;
C3	270	478	17.8 ±1.8 (12.8-20.8)	Humic-like, highly processed terrestrial; refractory, oxidized quinone-like	Stedmon & Markager, 2005; Yamashita et al. 2010
C4	305/ 435	522	14.8 ±2.6 (9.4-22.3)	Not commonly reported, similarities to fulvic-like, contributed from soils	Lochmuller & Saavedra, 1986; Stedmon et al., 2003
C5	325	442	9.8 ±3.5 (0.0-15.9)	Aquatic humic-like terrestrial; autochthonous, microbial produced; may be photoproduced	Boehme & Coble, 2000; Coble et al. 1998; Stedmon et al., 2003
C6	285	338	3.4 ±2.5 (0.0-9.3)	Amino acid-like/ Tryptophan-like. Freshly added from land, autochthonous. Rapidly photodegradable	Murphy et al. 2008; Shutova et al. 2003; Stedmon et al. 2007; Yamashita et al. 2003

^a Mean ± stdev (min-max) from all samples